

CHEMISTRY

AN **ASIAN** JOURNAL

www.chemasianj.org

Accepted Article

Title: New Promising Method for the Challenging Synthesis of 5-Acyl-2-Amino-3-Cyanothiophenes: Chemistry and Fluorescent Properties

Authors: Kseniya I. Lugovik, Alexander K. Eltyshev, Enrico Benassi, and Nataliya P. Belskaya

This manuscript has been accepted after peer review and appears as an Accepted Article online prior to editing, proofing, and formal publication of the final Version of Record (VoR). This work is currently citable by using the Digital Object Identifier (DOI) given below. The VoR will be published online in Early View as soon as possible and may be different to this Accepted Article as a result of editing. Readers should obtain the VoR from the journal website shown below when it is published to ensure accuracy of information. The authors are responsible for the content of this Accepted Article.

To be cited as: *Chem. Asian J.* 10.1002/asia.201700721

Link to VoR: <http://dx.doi.org/10.1002/asia.201700721>

A Journal of



A sister journal of *Angewandte Chemie*
and *Chemistry* – A European Journal

WILEY-VCH

FULL PAPER

New Promising Method for the Challenging Synthesis of 5-Acyl-2-Amino-3-Cyanothiophenes: Chemistry and Fluorescent Properties

Kseniya I. Lugovik,^[a] Alexander K. Eltyshv,^[a] Enrico Benassi,^{*[b]} Nataliya P. Belskaya^{*[a]}

Abstract: Independent of the substrate structure and reaction conditions, 2-cyano-3-aminothioacrylonitriles, which contains two active electrophilic centers, were shown to interact with various active halo methylene compounds under mild conditions to afford 5-acyl-2-amino-3-cyanothiophenes as the only products. A series of new polyfunctional thiophene derivatives with a rare combination of functionalities were synthesized and their photophysical properties were experimentally and computationally investigated. The calculated electronic characteristics of the ground and excited states were compared to the experimental results, which provided a good understanding of the relationship between the optoelectronic properties and the molecular structures. After absorption of light quanta, the systems populate an intramolecular charge transfer (ICT) Franck-Condon state, and emission occurs from a twisted ICT (TICT) minimum.

Introduction

The thiophene ring is an attractive core among five-membered heterocycles due to their broad use in various fields. Thiophenes are a classical bioisostere for the benzene ring in medicinal chemistry.^[1] Many molecules bearing a thiophene ring exhibit important pharmacological activities.^[1,2] Some of these molecules are biologically active natural compounds and plant pigments.^[1] Due to their unusual electronic nature and low aromaticity,^[1,2] thiophenes are an ideal molecule for applications in polymers, liquid crystals and dyes which find wide applications in material science^[1,3] and coordination chemistry.^[4] Thiophene and polythiophene are also efficiently applied as π -bridges, which improves the molecular hyperpolarizability of the push-pull systems.^[5] Unsubstituted thiophene and bithiophene are not capable of emission,^[1] and limited examples of thiophene derivatives (functionalized mono- or bithiophenes) with fluorescent properties have been reported.^[6] Fluorescence of heterocyclic systems including thiophenes rings typically arises

from the presence of additional fluorogenic heterocycles in their structure.^[7] In addition, the design and synthesis of new small molecule fluorophores with a required set of functionalities or substituents is interesting for understanding this phenomenon, extending the fluorescent compound set, and broadening their application in medicine and biology.

The classical approaches for the synthesis of substituted thiophenes are based on subsequent functionalization of the thiophene ring or condensation reactions, which directly afford polyfunctionalized thiophenes.^[1,2a,8] Stepwise modification of the thiophene nucleus often consists of a prolonged, multistep process.^[2a] Additionally, the introduction of specific functionalities (CN-group) or combinations of functionalities using this approach is a challenge in thiophene chemistry. Furthermore, the synthesis of thiophenes bearing acyl and amino group is also difficult. The conventional method for regioselective formation of substituted thiophenes that starts from acyclic precursors is based on heterocyclization of functionalized alkynes.^[8a,b] Nevertheless, this method provides mainly alkyl- or aryl-substituted thiophenes and only limited types of functionalized derivatives (e.g., alkoxy-carbonyl). The most convenient method for preparing thiophenes is the well-known Gewald method.^[8b] This method is the most suitable route for obtaining 2-aminothiophenes, which are useful intermediates in the preparation of dyestuffs and pharmaceuticals.^[2a] However, this methodology is typically associated with several drawbacks including harsh reaction conditions as well as complex and tedious experimental procedures, and limited yields are often obtained. A promising alternative consists of a one-step straightforward method for the synthesis of highly functionalized thiophene scaffolds based on the heterocyclization of thioacetamide derivatives bearing additional electrophilic centers with bromoketones.^[8] According to this mechanism, the typical transformation involves the cyclization of arylhydrazonothioacetamides **1**, which affords a series of 1-acyl-3-amino-4-arylazo-5-*tert*-cycloalkylaminothiophenes **4** (Scheme 1).^[8d,e]

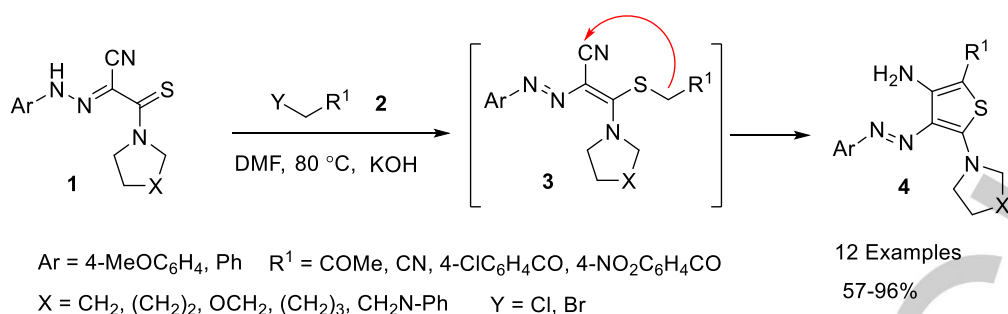
However, 3-cyclohexylamino-3-cyanopropenthioamide **6**, which is generated in situ from 3-morpholino-3-thioxopropane nitrile **5a** and cyclohexyl isocyanide, reacts with phenacyl bromides followed by the subsequent formation of 2-morpholino-5-arylothiophenes **8**. Scheme 2 outlines the route devised to prepare compounds **8** via formation of enamine **6B** followed by alkylation, cyclization and aromatization, which is accomplished by elimination of cyclohexylamine.^[8c]

[a] Kseniya I. Lugovik, Alexander K. Eltyshv, Prof. Nataliya P. Belskaya
Ural Federal University,
19 Mira Str., Yekaterinburg 620002 (Russian Federation)
E-mail: n.p.belskaya@urfu.ru

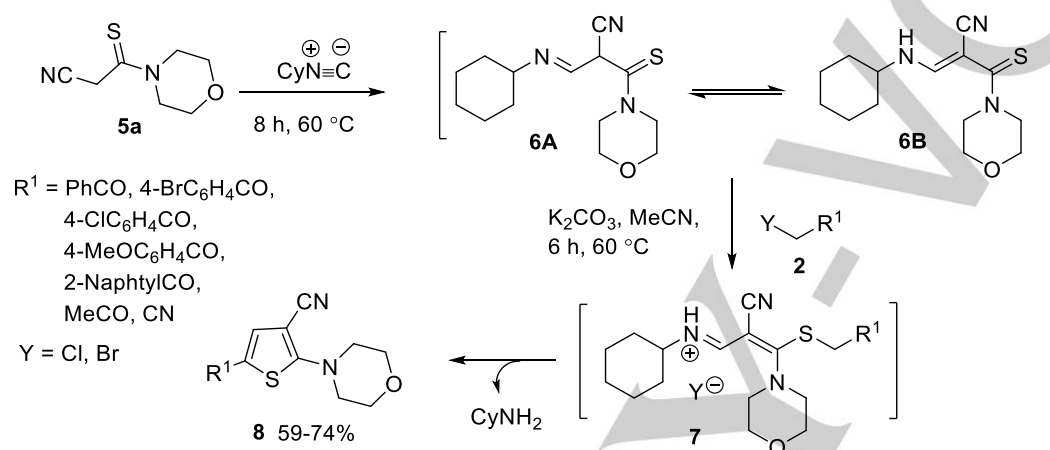
[b] Dr. Enrico Benassi
Scuola Normale Superiore,
Piazza dei Cavalieri 7 56126, Pisa (Italy)
E-mail: enrico.benassi@sns.it

Supporting information and the ORCID identification numbers for the authors for this article is given via a link at the end of the document.

FULL PAPER



Scheme 1.



Scheme 2.

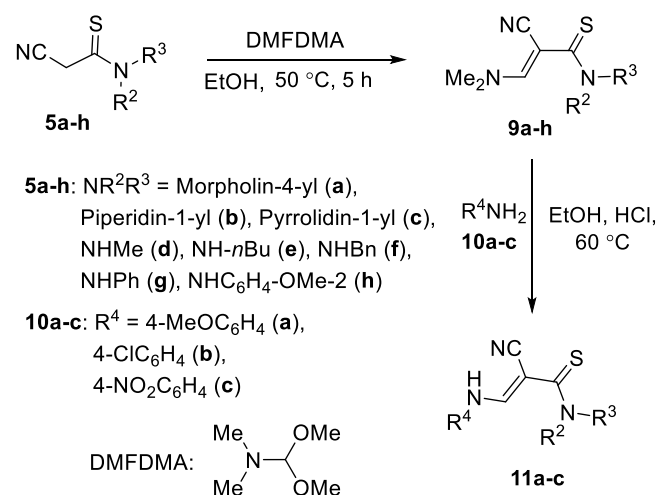
The investigation of this reaction with a wide range of α -haloketones, α -halonitrile, α -haloanilide and α -haloester allowed for the preparation of thiophenes with phenacyl bromides and chloroacetone nitrile.^[8c] However, 2-chloro-*N*-phenylacetamide and ethyl-2-chloroacetate failed to take part in this methodology.

The aim of this investigation was to elaborate this method for the synthesis of polyfunctionalized thiophenes involving various 3-aminothioacrylamides and different types of halogen compounds with activated methylene group, determine the potential for realizing two alternative synthetic mechanisms for their heterocyclization (Schemes 1 and 2), and estimate the scope and limitation of the investigated process. Therefore, we designed the structure of the starting compounds along with the synthetic tasks. The synthesized thiophene compounds were subsequently characterized to determine their spectroscopic and photophysical properties.

Results and Discussion

Availability, variability, safety, and environmental impact of starting compounds are important factors to consider during the design of a synthetic methodology. Cyanides (Scheme 2) are very toxic and volatile compounds and difficult to synthesize. Alternative reagents may include aminothioacrylamides, which are readily accessible by a variety of different methods.^[9] For their

synthesis, we chose a two-step procedure based on the condensation of readily available cyanothioacetamides^[9a,10] with dimethylformamide dimethylacetal (DMFDMA) followed by nucleophilic substitution of the dimethylamine moiety by the desired secondary or tertiary amines (Scheme 3, Table 1). The method for the synthesis of the arylaminothioacrylamides was previously described and verified.^[9c]



Scheme 3.

For internal use, please do not delete. Submitted_Manuscript

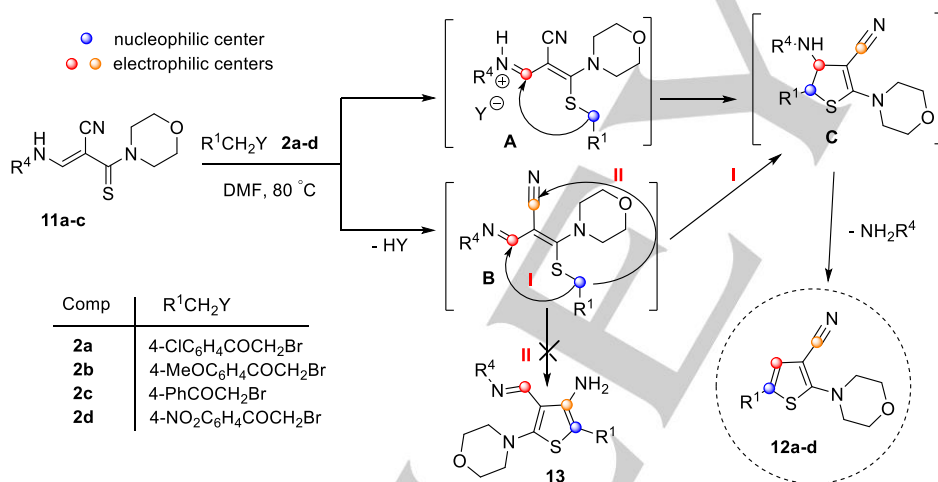
FULL PAPER

Table 1. Conversion time and yields for the synthesis of aminothioacrylamides **9a-h** and **11a-c**.

Entry	Comp	NR ² R ³	NMe ₂ /HNR ⁴	Time [h]	Yield ^[a] [%]
1	9a	Morpholin-4-yl	NMe ₂	2.0	75
2	9b	Piperidin-1-yl	NMe ₂	2.0	86
3	9c	Pyrrolidin-1-yl	NMe ₂	2.0	92
4	9d	NHMe	NMe ₂	2.0	65
5	9e	NH- <i>n</i> Bu	NMe ₂	3.0	67
6	9f	NHBn	NMe ₂	2.0	84
7	9g	NHPh	NMe ₂	2.0	57
8	9h	2-MeOC ₆ H ₄	NMe ₂	4.0	50
9	11a	Morpholin-4-yl	4-MeOC ₆ H ₄	3.0	75
10	11b	Morpholin-4-yl	4-ClC ₆ H ₄	2.5	65
11	11c	Morpholin-4-yl	4-NO ₂ C ₆ H ₄	3.0	87

[a] Isolated yields after purification.

Newly synthesized compounds **9d-h** and **11a-c** were characterized by elemental analyses, MS and NMR. These data, which are provided in the Supplementary Information (SI, Figures S1-11), are consistent with the suggested structures. It is important to note that compounds **11** were isolated as a mixture of *Z*- and *E*-isomers.

**Scheme 4.****Table 2.** Reaction of 3-aminothioacrylamides and **11a-c** with phenacyl bromides **2a-d**.

Entry	Comp 11	R ⁴	Comp 2	Comp 12	R ¹	Time [h]	Yield 12 ^[a] [%]
1	11a	4-MeOC ₆ H ₄	2a	12a	4-ClC ₆ H ₄ CO	0.5	87
2	11b	4-ClC ₆ H ₄	2a	12a	4-ClC ₆ H ₄ CO	0.5	94
3	11c	4-NO ₂ C ₆ H ₄	2a	12a	4-ClC ₆ H ₄ CO	1.5	85
4	11b	4-ClC ₆ H ₄	2b	12b	4-MeOC ₆ H ₄ CO	1.0	93
5	11b	4-ClC ₆ H ₄	2c	12c	4-C ₆ H ₅ CO	1.0	62
6	11b	4-ClC ₆ H ₄	2d	12d	4-NO ₂ C ₆ H ₄ CO	2.5	63

[a] Isolated yields after purification.

For internal use, please do not delete. Submitted_Manuscript

FULL PAPER

The ^1H and ^{13}C NMR spectra, mass spectra, and FTIR spectra were consistent with the expected structures for compounds **12a-d** (See Experimental part and SI, Figures S12-15). In the mass spectra of compounds **12a-d**, peaks for molecular ions with 46-100% relative intensity were readily observed. All 5-aryloxy-carbonyl-substituted 2-aminothiophenes **12a-d** exhibited bands at 1600-1642 ($\text{C}=\text{O}$) and 2208-2215 cm^{-1} (CN) in their FTIR spectra. The positions of these bands are not typical for CN and CO bond stretching and may be due to their strong conjugation with the thiophene ring. The ^{13}C NMR spectra contained common signals corresponding to carbon atoms in the carbonyl group, CN groups and C4H thiophene ring at 169.3-169.9 ppm, 114.4-117.0 ppm and 136.9-149.0 ppm, respectively. The extreme shift in the CO signal to high field suggests strong conjugation with the heterocyclic scaffold. This interpretation of the spectral data was subsequently supported by quantum mechanical calculations (*vide infra*).

To highlight the differences in the two possible reaction curves (via stage I or stage II) for reagents **11a** and **2a**, we performed quantum chemical calculations using density functional theory (DFT) and accounted for solvent effects (DMF) using IEF-PCM (cf. Computational Details). The charge distribution and electrostatic potential for all compounds (*viz.*, reactants, intermediates, and products) and the difference in the thermochemical quantities (including the Gibbs free energies) for the reactions including the last stage (I) leading to thiophene **12a** (ΔG_{I}) and reaction with the last stage (II) leading to thiophene **13a** (ΔG_{II}) were calculated (SI, Scheme S1). The ESP charge distribution analysis (SI, Figure S37, Table S3) demonstrates that the largest amount of charge was localized on carbon atom C_{CN} ($q = 0.527 e$), and this value should be compared to carbon atom C_{CH} of the enamine moiety ($q = 0.365 e$), which confirms the significant decrease in its susceptibility to nucleophilic attack atom C_{CH_2} . However, the electrostatic potential values for these atoms are much closer (-14.755 and -14.729 a.u. for atoms C_{CN} and C_{CH} , respectively) (SI, Table S3). The appreciably negative $\Delta G_{\text{I}} = -42.0 \text{ kJ/mol}$ for the transformation of **11a** and **2a** to **12a** compared to $\Delta G_{\text{II}} = -30.4 \text{ kJ/mol}$ for the same transformation to **13a** indicates that the formation of thiophene **12a** is the most thermodynamically favorable (SI, Table S1). Therefore, the reaction was under thermodynamic control and followed direction I to more stable thiophenes **12**.

A very useful descriptor for determining the sites for nucleophilic/electrophilic attack is a map of the molecular electrostatic potential (MEP).^[11] The MEP (Figure 1 a) provides a visual representation of the chemical active sites and comparative reactivity of atoms. The potential value increases according to a continuum scale of colors from red (negative) to blue (positive). In our case, negative regions in the MEP corresponded to electrophilic reactive centers, and positive regions corresponded to nucleophilic reactive centers. The MEP was calculated for intermediate **B** and indicated that the C_{CN} atom is the most electrophilic site. In addition, the C_{CH_2} atom was the most nucleophilic site (Figure 1 a).

The optimized geometry of intermediate **B** (Figure 1 b) possessed a C_{CH_2} and C_{CH} (3.112 Å) distance that was shorter than that between another pair of electrophile and nucleophile centers ($\text{C}_{\text{CH}_2}\text{-C}_{\text{CN}} = 5.120 \text{ Å}$). Such rapprochement of the two active sites can be explained by the presence of a weak

intramolecular interaction between the sulfur atom and the nitrogen atom of the enamine group ($I_{\text{S}\cdots\text{N}} = 3.005 \text{ Å}$, the sum of van der Waals radii for these atoms is $R_{\Sigma\text{vdW}(\text{S-N})} = 3.355 \text{ Å}$). The presence of this interaction was confirmed by the RDG plot (Figure 1 c),^[12] which is a state-of-the-art technique based on the electron density that is particularly reliable for investigating weak interactions.

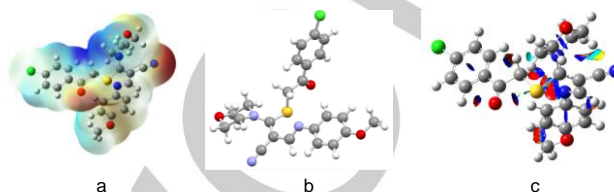


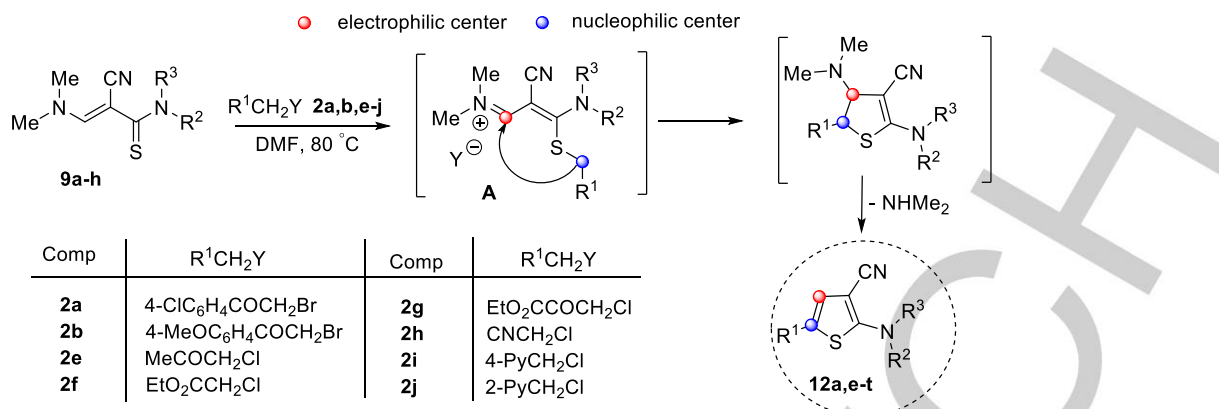
Figure 1. Intermediate **B** (in solution of DMF). (a) MEP; (b) optimized geometry; (c) RDG plot. Legend of MEP colors: red (negative potential) and blue (positive potential). Legend for the elements: hydrogen (white), carbon (grey), nitrogen (blue), and oxygen (red).

The synthetic results indicate the preferred participation of the carbon atom in the $=\text{CHNHAr}$ group and exclusion of the CN function from the heterocyclization process. This behavior indicates that the reaction mechanism is independent of the substituent at the amino moiety in 3-aminopropene thioamides **11a-c**. Therefore, further investigations involved only the use of 3-aminothioacrilamide **9a-i** with a $=\text{CHNMe}_2$ group. These substrates provide the best reactivity due to the formation of intermediate **A** (Scheme 4 and 5) and represent the most convenient solution in term of atom economy and technological arrangement of the process due to the elimination of a smaller and more easily separated dimethylamine molecule with respect to 4-chloraniline or 4-anisidine during the reaction.

Next, we used the optimal reaction conditions (DMF, 80 °C) to synthesize a series of new functionalized thiophenes (Table 3). To investigate the scope of this reaction, we employed a range of halocarbonyl compounds **2a,b,e-g**, 2-chloroacetonitrile **2h**, pycolyl chlorides **2i,j**, and along with the 3-morpholinoderivatives, we employed thioamides **9b-h** with other *tert*-cycloalkylamino and different secondary amino groups. Most of the condensed reagents **2** afforded the desired thiophenes with satisfactory yields and short reaction times. It is important to note that a decrease in the activity of the CH_2 group in halomethylene compounds **2e-j** and the use of chloro derivatives slow down the process. Further improvement in the protocol was achieved by addition of 1 equivalent of TEA (Table 3, entries 12-17) for all these cases.

Most of the heterocyclic compounds described herein are new compounds whose structures were unambiguously confirmed using elemental analysis, NMR, FTIR spectroscopy (Experimental section and SI, Figures S16-31) and mass spectrometry. The thiophenes were obtained as yellowish solids. Their solutions in organic solvents exhibit fluorescence under irradiation with UV light. (SI, Figures S45-47).

FULL PAPER



Scheme 5. Conditions: a - DMF, 80 °C; b – DMF, 1 equiv. TEA, 80 °C

Table 3. Reaction of 3-aminothioacrylamides **9a-h** with halo methylene compounds **2a,b,e-j**.

Entry	Comp 9	NR ² R ³	Comp 2	Comp 12	R ¹	NR ² R ³	Time [h]	Yield ^[a] 12 [%]
1	9a	Morpholin-4-yl	2a	12a	4-ClC ₆ H ₄ CO	Morpholin-4-yl	0.5	94
2	9b	Piperidin-1-yl	2b	12e	4-MeOC ₆ H ₄ CO	Piperidin-1-yl	0.5	90
3	9c	Pyrrolidin-1-yl	2b	12f	4-MeOC ₆ H ₄ CO	Pyrrolidin-1-yl	0.5	80
4	9c	Pyrrolidin-1-yl	2a	12g	4-ClC ₆ H ₄ CO	Pyrrolidin-1-yl	0.5	67
5	9d	NHMe	2b	12h	4-MeOC ₆ H ₄ CO	NHMe	0.5	87
6	9d	NHMe	2a	12i	4-ClC ₆ H ₄ CO	NHMe	0.5	62
7	9e	NH <i>n</i> Bu	2a	12j	4-ClC ₆ H ₄ CO	NH <i>n</i> Bu	0.5	72
8	9f	NHBn	2a	12k	4-ClC ₆ H ₄ CO	NHBn	0.5	93
9	9g	NHPh	2a	12l	4-ClC ₆ H ₄ CO	NHPh	0.5	96
10	9g	NHPh	2b	12m	4-MeOC ₆ H ₄ CO	NHPh	1.0	72
11	9h	2-MeOC ₆ H ₄	2a	12n	4-ClC ₆ H ₄ CO	2-MeOC ₆ H ₄	0.5	84
12	9a	Morpholin-4-yl	2e	12o	MeCO	Morpholin-4-yl	0.5 ^[b]	78
13	9a	Morpholin-4-yl	2f	12p	EtOOC	Morpholin-4-yl	1.0 ^[b]	56
14	9a	Morpholin-4-yl	2g	12q	EtOCCO	Morpholin-4-yl	1.0 ^[b]	84
15	9a	Morpholin-4-yl	2h	12r	CN	Morpholin-4-yl	1.0 ^[b]	83
16	9a	Morpholin-4-yl	2i	12s	Pyridin-4-yl	Morpholin-4-yl	1.0 ^[b]	92
17	9a	Morpholin-4-yl	2j	12t	Pyridin-2-yl	Morpholin-4-yl	2.0 ^[b]	93

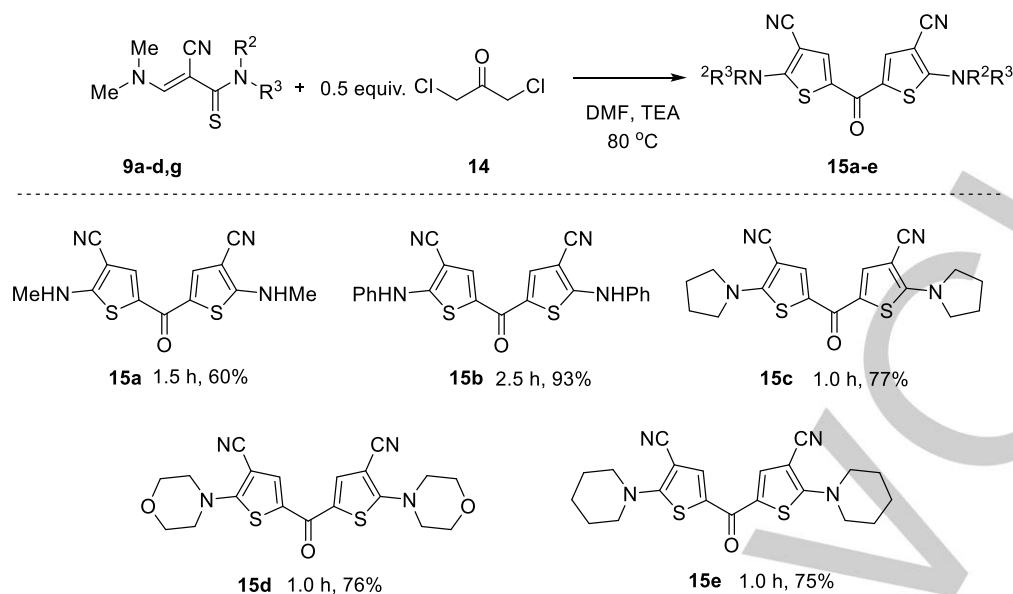
[a] Isolated yields after purification. [b] Reaction carried out with 1 equiv. TEA.

The range of applicability of the reported method was extended to the synthesis of bithienoketones **15a-e** using dichloroacetone under ambient conditions for condensation with thioamides **9a-d,g**. The reactions performed well with satisfactory rates and product yields (Scheme 6). The ¹H NMR spectra for newly synthesized compounds **15a-e** contain characteristic signals for all the proton-containing groups. The ¹³C NMR spectra are shown

in Figures S32-36 (SI). The carbonyl carbon atom signal was located at 164.9-173.7 ppm, the thiophenes C4H carbon signal was located at 134.8-136.9 ppm, and the signal at 112.3-116.7 ppm was due to the CN carbon atom. Details of the experimental procedures and data for structural characterization are provided in the Experimental Section as well as the Supporting Information (SI).

For internal use, please do not delete. Submitted_Manuscript

FULL PAPER



Scheme 6.

UV-Vis Absorption and Fluorescence Spectra

The photophysical properties of prepared compounds **12a-t** and **15a-e** were investigated using UV-Vis and fluorescence spectroscopy in dioxane at room temperature (Table 4 and Figure 2). The UV-Vis spectra of thiophenes **12a-t**, **15a-e** exhibit a λ_{\max} in the range of 321–418 nm (Table 4). The molar extinction coefficients indicate that the main band in the absorption spectra resulted from population of a charge transfer state, which was primarily due to a $\pi \rightarrow \pi^*$ transition. The change in the nature of the substituent in the aroyl group at the C5_{Thioph} position does not significantly affect the absorption spectrum, and a small shift in the longest wavelengths from 361 nm to 377 nm (1176 cm^{-1}) was observed (Table 4, entries 1–4, Figure 2 a). In contrast, replacement of the aroyl group at the C5 thiophene carbon atom to acetyl, ethoxycarbonyl, and CN groups resulted in a dramatic hypsochromic effect for the longest wavelengths (Table 4, entries 15–18, Figure 2 e). In addition, introduction of 2- or 4-pyridine at the C5 thiophenes ring causes the same effect (Table 4, entries 19, 20). Notably, bithienoketones **15a-e** result in a redshift of the longest wavelengths (Table 4, entries 21–25) in the 383–418 nm region (Figure 2 g).

The fluorescence spectra of all the studied compounds exhibit a maximum wavelength for emission at 400–475 nm as well as blue and blue-green light emission. The emission spectra of compounds **12i-k,n,p,q,s** exhibited dual fluorescence and were broadened, especially for compound **12j** and **12n** (HWHM = 5759 and 6208 cm^{-1} , respectively). The dual fluorescence of these types

of compounds is related to the equilibration between two conformers (i.e., the former has a twisted geometry, and the latter has a planar geometry).^[13]

Similar to the UV-Vis absorption spectra, the fluorescence spectra and their efficiencies can also be tuned by substituents on positions 2 and 5 of the thiophene ring. Changes in the substituents in the para position of the aroyl C5_{Thioph} fragment as well as the type of amine group in the C2 thiophene affect the emission spectra and quantum yields. For example, the presence of a 4-NO₂-benzoyl moiety at the heterocycle C5 atom quenches the efficiency of the emission (Table 4, entry 4). High quantum yield values were obtained for thiophenes **12b,e,f,m** (Table 4, entries 2,5,6,13). Therefore, structures including a 4-methoxybenzoyl substituent may stabilize the excited state and enhance the probability for electron transition. The structure of the amine group attached to C2 thiophene is also important for the fluorescence intensity. The presence of a *tert*-cycloalkylamino or phenyl amino group enhances the fluorescence quantum yield.

It is important to note that an increase in the quantum yields of bithienoketones **15a,c-e** occurs along with a small bathochromic shift and blue-green fluorescence (Table 4, entries 21–25 and Figure 1 d). The largest Stokes shifts was observed for thiophenes **12a,l,n,q** and bithienoketone **15b**. As observed in related structures, this phenomenon indicates large differences between the Franck-Condon state and the relaxed adiabatic minimum from which the emission occurs.

FULL PAPER

Table 4. Photophysical properties of compounds **12a-t** and **15a-e** in 1,4-dioxane.

Entry	Comp	λ_{abs} [nm]	ϵ_{max} [M ⁻¹ ·cm ⁻¹]	λ_{em} [nm]	Φ_F [a] [%]	HWHM [b] [cm ⁻¹]	Stokes shift [nm/cm ⁻¹]
1	12a	365, 254	22645, 13358	456	1.53	3175	91/5467
2	12b	361, 286	22347, 11514	441	6.62	2737	80/5025
3	12c	362, 285	21311, 5807	450	1.58	3051	88/5402
4	12d	377, 259	24386, 17150	- ^[c]	-	-	-
5	12e	367, 286	21311, 12582	442	7.78	2623	75/4624
6	12f	371, 284	26271, 13320	441	6.40	2623	70/4248
7	12g	374, 250	24146, 12582	460	0.90	3293	86/4999
8	12h	385, 281	26658, 13318	432	0.90	3097	86/4999
9	12i	362, 281, 249	26148, 3828, 9823	408, 448	1.64	4490	46/2826
10	12j	363, 249	22745, 12016	415, 447	0.80	5759	84/5177
11	12k	362, 250	21970, 10925	415, 449	0.80	4672	87/5353
12	12l	374	11584	465	4.04	3314	91/5233
13	12m	371, 291	23524, 13628	451	3.77	3409	80/4781
14	12n	373	20776	423, 462	0.30	6208	89/6312
15	12o	344, 285	18847, 5564	400	0.65 ^[d]	3045	56/4070
16	12p	326, 286	19348, 6200	387(sh), 405	0.31 ^[d]	2690	79/5983
17	12q	378, 286	15655, 5089	432, 468	0.23	4130	90/5088
18	12r	321	14979	400	2.33 ^[d]	3199	79/6153
19	12s	345, 281	20385, 16599	388, 404	0.64	4269	59/4233
20	12t	348, 293	20345, 6835	409	1.85	3097	61/4286
21	15a	395, 329, 283	12115, 8335, 8807	451	3.1	2261	56/3144
22	15b	383, 294	13018, 9830	475	1.2	2215	92/5057
23	15c	418, 360, 291	30617, 6311, 10953	465	3.9	2087	47/2418
24	15d	403, 291	12248, 4560	465	3.9	2147	61/2418
25	15e	412	24311	468	3.3	2020	56/2904

[a] - The fluorescence quantum yields (Φ) were estimated with quinine sulfate (Φ_F) 0.55 in a 1 N H₂SO₄ solution as a standard, λ_{ex} = 366 nm (5×10^{-6} M) (dioxane, 5×10^{-6} M).^[14] [b] - Half-Width at Half Maximum. [c] - No emission. [d] - The fluorescence quantum yields (Φ_F) were estimated with anthracene (Φ_F) as a standard, λ_{ex} = 376 nm (solvent in EtOH).^[14]

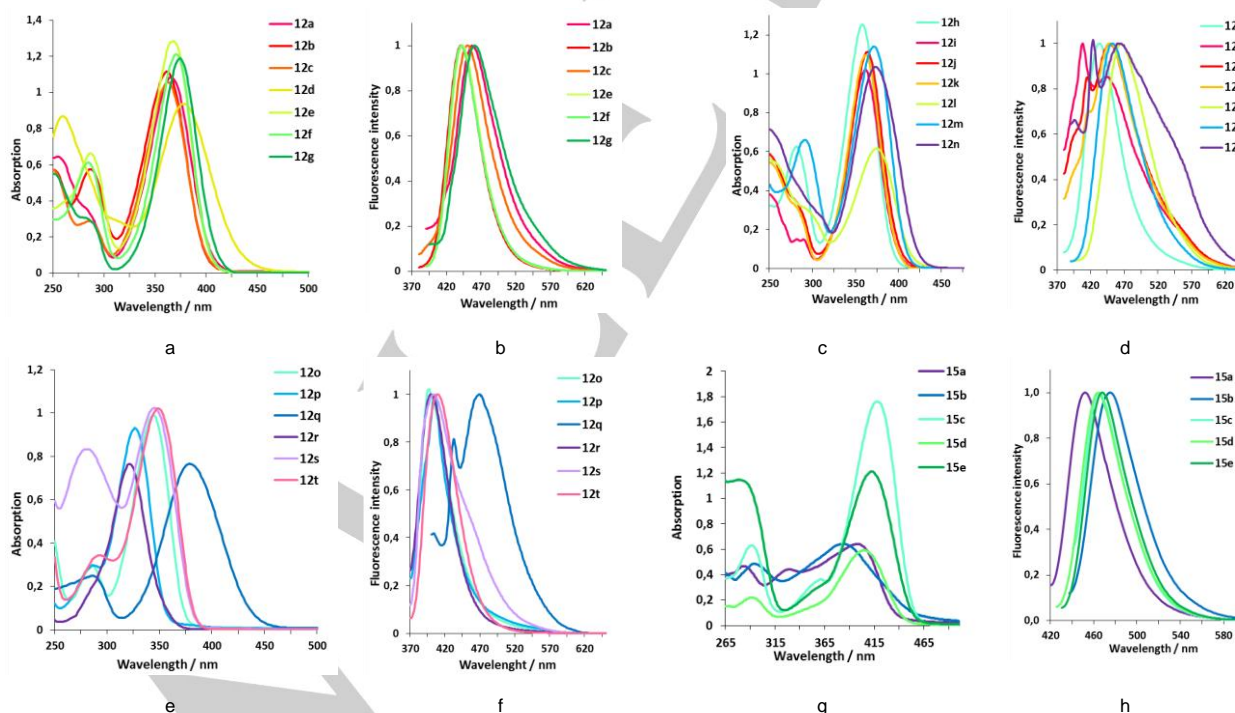


Figure 2. Absorption ($c = 5 \times 10^{-5}$ M) and normalized fluorescence spectra ($c = 5 \times 10^{-6}$ M) of thiophenes **12a-g** (a,b), **12h-n** (c,d), **12o-t** (e,f) and bithienoketones **15a-e** (g,h) in 1,4-dioxane at room temperature.

For internal use, please do not delete. Submitted_Manuscript

FULL PAPER

New thiophene derivatives **12** and **15** exhibit good solubility in common polar and non-polar organic solvents, such as *n*-hexane, 1,4-dioxane, toluene, chloroform, acetone, acetonitrile, alcohols, DMF and DMSO. To evaluate the effect of the solvent polarity on the absorption and emission of the synthesized thiophenes, the spectra of compounds **12a,b** were measured in solvents with

different polarities (Table 5, Figure 3). The (fluoro)solvatochromic results indicate that a long-wavelength absorption band is located in the 355 to 374 nm region in more polar solvents. Thiophenes **12a** and **12b** absorb in the UV-Vis region between 355 and 374 nm and 359 and 370 nm, respectively.

Table 5. Absorption and emission maxima, quantum yield and Stokes shift of thiophenes **12a** and **12b** in different solvents at room temperature.

Entry	Comp	Solvent	λ_{abs} [nm]	ϵ_{max} [M ⁻¹ ·cm ⁻¹]	λ_{em} [nm]	Φ_F [a] [%]	HWHM ^[b] [cm ⁻¹]	Stokes shift [nm/cm ⁻¹]
1	12a	Hexane	355, 255, 212	21461, 13254, 24244	439	0.74	3454	84/5390
2		Toluene	365	26052	450	2.17	2982	85/5175
3		1,4-Dioxane	365, 254	22645, 13358	456	1.53	3175	91/5467
4		CHCl ₃	365	25325	460	1.05	3478	95/5658
5		AcOEt	364	22520	421, 464	0.52	3475	100/5921
6		CH ₂ Cl ₂	367, 356	18596, 10360	417, 464	0.73	3571	97/5696
7		DMSO	374	23430	433	0.48	3729	59/3643
8		<i>n</i> PrOH	367, 257, 213	22991, 13296, 26112	416, 459	0.40	3806	92/5462
9		DMF	371	21363	424, 475	0.20	4839	104/5902
10		EtOH	368, 256, 210	22832, 13961, 28483	423, 463	0.23	4411	95/5576
11	12b	MeCN	368, 253	21707, 12060	421, 466	0.14	5485	98/5714
12		Aceton	366	22828	422, 475	0.24	3695	109/6270
13		THF	365, 252	22828, 13860	416, 463	1.00	3888	98/5799
14		Toluene	360	21623	431	6.47	2737	71/4576
15		1,4-Dioxane	361	22347	441	6.62	2656	80/5025
16		CHCl ₃	361	24055	442	6.11	2757	81/5076
17		AcOEt	359	20484	443	3.69	2757	84/5282
18		DMSO	370	19303	461	1.84	2989	91/5335
19		DMF	364	20744	455	3.02	3204	91/5495
20		EtOH	364	20435	455	0.73	3245	91/5495
21		MeCN	363	20153	456	1.04	3026	93/5618
22		Acetone	361	19950	451	2.54	2856	90/5528
23		<i>n</i> PrOH	363	21547	450	1.72	3065	87/5326
24		THF	360	23287	443	4.91	2737	83/5204

[a] - The fluorescence quantum yields (Φ) were estimated with quinine sulfate (Φ_F) 0.55 in a 1 N H₂SO₄ solution as a standard, λ_{ex} = 366 nm (5×10^{-5} M) (dioxane, 5×10^{-6} M).^[14] [b] - Half-Width at Half Maximum.

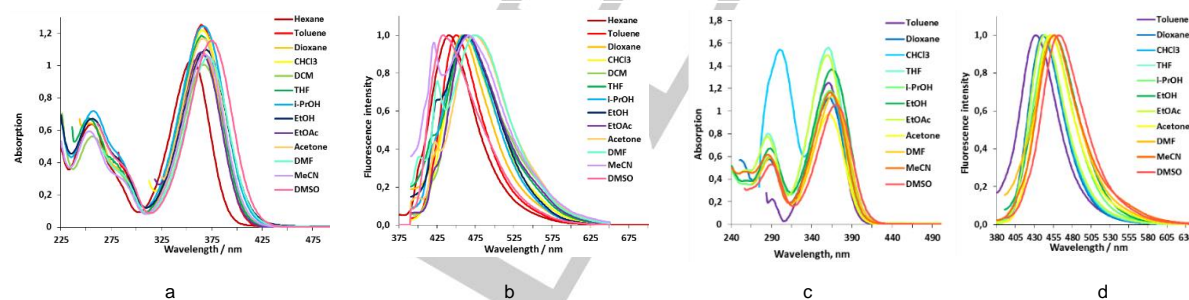


Figure 3. UV-Vis absorption (5×10^{-5} M) and normalized fluorescence spectra (5×10^{-6} M) of thiophenes **12a** (a,b) and **12b** (c,d) in different solvents at room temperature.

Although the absorption spectra are slightly dependent on the solvent polarity (shift of 995 and 1432 cm⁻¹ for **12a** and **12b**, respectively), the emission spectra exhibit more remarkable fluorosolvatochromic effects (2042 and 1510 cm⁻¹ for **12a** and **12b**, respectively), which suggests that emission is occurring from an ICT minimum in the excited state. The extent of the solvatochromic shift strongly depends on the nature of the substituent on the aryl group. The increasingly red-shifted emission may be due to the higher electron acceptor strength of the Cl substituent and an increased degree of charge transfer

upon photoexcitation. Compounds **12a** and **12b** exhibit remarkable Stokes shifts in the 3643-6270 cm⁻¹ and 4576-5618 cm⁻¹ ranges, respectively. The largest Stokes shifts for thiophenes **12a,b** were observed in polar solvents (i.e., acetone and acetonitrile, respectively), which supports the hypothesis that an ICT transition occurs during the photoexcitation. The fluorescence intensity is very sensitive to the solvent polarity for compound **12a** and **12b**. The quantum yields for **12a** and **12b** were in the 0.14-2.17% and 0.73-6.62% ranges, respectively. For compound **12a**, in addition to the principal band, an additional band in the 416-

For internal use, please do not delete. Submitted_Manuscript

FULL PAPER

423 nm range was observed when the spectra were recorded in polar solvents (i.e., MeCN, AcOET, EtOH, THF, *i*PrOH, DMF, acetone and DCM), suggesting that highly polar solvents favor rotational isomerization of the substrate to a polar TICT minimum (Figure 3 b).

Quantum mechanical calculations

To confirm the trends revealed by the experimental investigations and their interpretation, quantum mechanical calculations were performed using time-dependent density functional theory (details are provided in the dedicated section) for a number of

representative thiophenes (i.e., **12a-d,i,l,m,n,s,t** and **15a,d**). Notably, most of the synthesized thiophenes (**12** and **15**) may exist as a mixture of several conformers (Figure 4 and more additional examples in SI, Figure S38). After studying the rotameric equilibria, the same global minimum rotamer was revealed within the same group of compounds. For example, the *cis*-SO rotamer (i.e., **B**) with a C=O group and S-atom of the heterocycle ring in a *cis* conformation was predicted to be the most stable form for thiophenes **12a-d**. For the bithienoketones, the S-atom in the thiophene ring (*cis*-SO-*trans*-S) of the most stable rotamer (i.e., **B**) has the opposite orientation. The stabilization is supported by the presence of weak attractive intramolecular interactions.

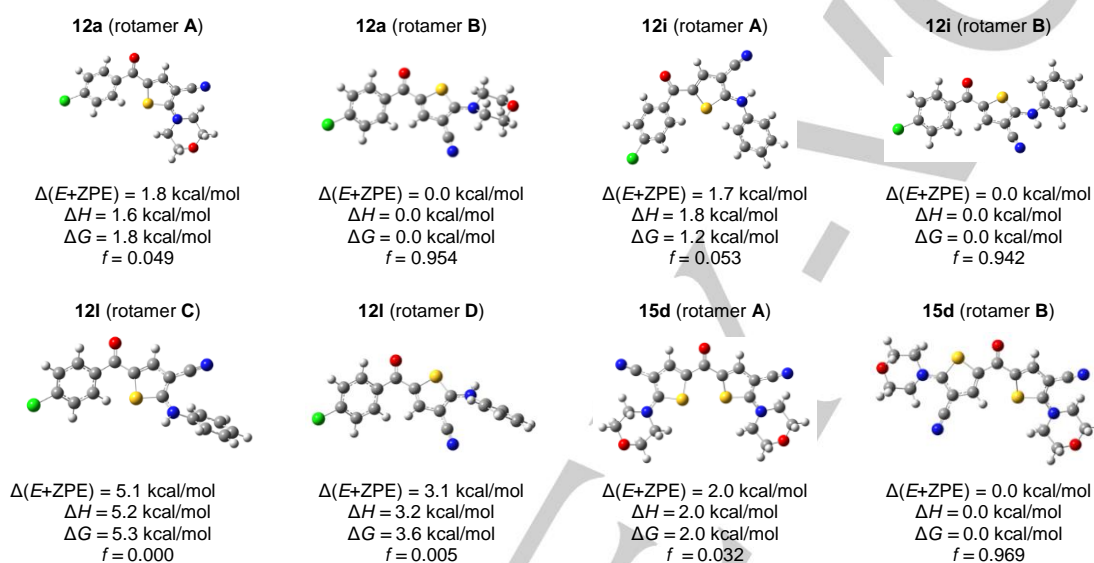


Figure 4. Rotameric study. Relative electronic energy plus zero point energy ($\Delta(E+ZPE)$), Gibbs free energy (ΔG), enthalpy (ΔH) and Boltzmann factor (f) computed at 300 K for ground state of possible thiophene rotamers in 1,4-dioxane. Level of theory: DFT M06-2X (SMD) / aug-cc-pVTZ.

The preference for the same rotamer was confirmed in other solvents (i.e., DCM, acetone, MeCN, and DMSO). The origin of the stability of the different rotamers was investigated by analysing the intramolecular interactions via a reduced density gradient (RDG)^[12] for compounds **12a,b,g,n,s,t**, and **15a** (SI, Figure S39). Within thiophene molecules, various weak intramolecular interactions were detected, and these interactions are responsible for the stabilization of the rotamers and affect the vibronic relaxation after excitation. The strongest of these interactions was observed between the aromatic and thiophene rings, which stabilizes the *cis*-conformation of the C=O group and S-atom of thiophenes **12** and **15** (SI, Figure S39).

In addition, we investigated the stabilization of rotamer **B** for derivatives **12a-d,i,l-n** and **15d** in the ground (S_0) and excited (S_1) states. The RDG analysis confirmed a series of internal interactions (SI, Figure S39) that are responsible for this particular conformation. Along with the $S \cdots H-C_{Morph}$ (2.922-2.959 Å) and $C=O \cdots H-C_{Ar}$ (2.571-2.656 Å) hydrogen bonds in the ground state, additional weak interactions were observed between the S-atom

of thiophene and the O-atom of the carbonyl group (2.922-2.950 Å) (SI, Tables S4-6). Hypervalent non-bonded interactions of a divalent sulfur atom and a nearby heteroatom were previously reported in organic compounds.^[15] The directionality of the interaction strongly suggests the importance of the orbital interaction between the interacting atoms for stability. For the $S \cdots O$ interactions, the stabilization primarily arises from the $n(O) \rightarrow \sigma^*(S)$ orbital interaction. The electrostatic nature of the 1,4-type $S \cdots O$ interactions between a positively charged S atom and a negatively charged carbonyl O atom was proposed by Burling and Goldstein.^[15c]

Any substituents that are attached to thiophenes (CN, NR^1R^2 , C=O) participate in conjugation and extend the π -network in the ground state. A small twist θ from planarity is also indicative of extended π -electron delocalization. Only an aromatic ring bound to the carbonyl fragment in the C5-position of thiophenes exhibits a significant deviation from planarity (30.3-37.7 degs; SI, Tables S4-6).

For internal use, please do not delete. Submitted_Manuscript

FULL PAPER

Remarkable changes occur when S_1 is populated upon excitation and relaxes towards the emissive minimum of the excited state PES. $S \cdots H-C_{\text{Morph}}$ becomes shorter in compounds **12a-d** (from 2.527-2.617 Å in S_0 to 2.475-2.484 Å in S_1) but elongates in compounds **12i,l,n** (from 2.453-3.030 Å in S_0 to 2.487-3.275 Å in S_1). The interaction between the S and O atoms weakens, which results in an increase in the interatomic distance (from 2.932-2.950 Å in S_0 to 3.328-3.357 Å in S_1). The exception is compound **12l**, where excitation leads to this weak interaction strengthening (from 2.922 Å in S_0 to 2.784 Å in S_1). In general, we

can conclude that photoexcitation leads to weakening of the intramolecular interactions in favor of a more twisted conformation in excited state S_1 than in the ground state. The dihedral angle between the aryl fragment and the thiophene ring increases (up to 82.2-86.1 degs) due to the electronic structure separating into two independent parts. It is important to note that the C=O bond lengths are shorter in the ground state than in S_1 (from 1.248 Å in S_0 to 1.290 Å in S_1 ; SI, Tables S5-7), which typically occurs due to a decrease in conjugation during the excitation.

Table 6. Calculated absorption and emission properties^[a] for most stable rotamer of thiophenes **12a-d,i,l,m,n,s,t** and **15d**.

Entry	Comp	c	λ_a [nm]	f_{01}	μ_0 [D]	μ_{1v} [D]	$\theta_{0,1v}$ [°]	c'	λ_e [nm]	Δv [kK]	f_{10}	μ_{1r} [D]	$\theta_{0,1r}$ [°]
1	12a	0.67978	365.9	0.4011	2.7	9.4	28.7	-0.69667	457.4	5.47	0.0216	9.4	28.7
2	12b	0.68518	362.1	0.5243	1.9	3.1	145.8	0.69371	442.3	5.01	0.0229	10.6	133.6
3	12c	0.61115	363.0	0.2759	6.3	5.0	118.6	0.69568	451.1	5.38	0.0114	5.0	118.6
4	12d	0.70446	378.1	0.1162	6.6	28.4	15.3	0.69983	898.9	13.93	0.0081	33.3	14.5
5	12i	0.66541	363.2	0.3538	3.9	9.7	20.9	-0.69621	448.9	5.26	0.0157	12.7	21.9
6	12l	0.69881	375.1	0.5522	3.5	11.5	19.6	-0.69868	466.7	5.23	0.0230	21.4	17.1
7	12m	0.69184	371.8	0.6457	4.5	5.1	111.6	0.68595	452.3	4.79	0.0930	11.2	65.1
8	12n	0.69999	373.2	0.5661	5.1	15.3	6.3	-0.69178	462.6	5.18	0.0012	19.0	7.8
9	12s	0.69876	346.4	0.4864	3.4	7.0	43.2	-0.69765	404.8	4.16	0.0056	9.2	38.9
10	12t	0.70017	348.9	0.5302	3.9	2.7	99.3	0.69620	410.1	4.27	0.0087	5.1	109.8
11	15d	0.70222	403.9	0.5471	4.0	4.6	27.9	-0.69781	464.6	3.23	0.0251	12.5	104.7

[a] Computed orbital's coefficient (c and c'), absorption wavelength (λ_a , nm), fluorescence wavelength (λ_e , nm), oscillator strength (f_{01} and f_{10}), modulus of the electric dipole moments of the ground state (μ_0 , D) and of the vertical FC excited state (μ_{1v} , D), angles formed by the dipole moment vectors ($\theta_{0,1v}$ and $\theta_{0,1r}$).

UV-Vis absorption and emission spectra of molecules **12a-d,i,l-n,s,t** and **15d** were computationally simulated in solvent (1,4-dioxane) at the TD-DFT level (SI, Figure S40). Excellent agreement between the computed wavelengths and the experiment values was obtained (Table 4,6). The $c_{\text{H-L}}$ coefficients confirm that the first absorption band is dominated by the HOMO \rightarrow LUMO transition.

The calculated oscillator strengths are larger for absorption than for emission. These results are in agreement with the experimental data and confirm that compounds **12b,l,m** and bithienoketone **15d** exhibit better fluorescence than **12d** and **12n**, which exhibit limited emissivity.

With regards to the thiophene polarity and how it changes after photoexcitation and relaxation on the excited state potential energy hypersurface, the molecular electric dipole moment exhibits a slight change after photon absorption in some cases (e.g., thiophenes **12c,m,t** and **15d**) but remarkable change in other cases (e.g., compounds **12a,b,d,i,l,n,s**). Furthermore, for most compounds, the electric dipole moment increases after geometry relaxation. Along with an increase in the polarity after photoexcitation (i.e., increase in the intensity of the dipole moment), thiophenes **12b,c,m,t** and bithienoketone **15d** exhibit a remarkable change in the dipole moment direction.

Interestingly, compound **12a** tends to preserve the same electric dipole moment value in the excited state when surrounded by a solvent of increasing polarity. This characteristic was observed in DCM, acetone, acetonitrile, and DMSO (SI, Table S7). This behavior indicates the difference between the charge distribution in the ground and excited states in the solute with stabilization of the excited state in polar solvents and provides support for a charge-transfer transition.^[13]

To better understand the nature of the excited state and the ICT process, the FMOs are shown in Figure 5 for compounds **12a,b,d,m,n,s** and **15d** (additional examples are presented in the SI, Figure S41). Based on these plots, the ICT nature of the transition is evident and explains the redshifted emissions for most of the thiophenes.

The HOMO of compounds **12a-d,i,l,m** are primarily localized on the thiophene moiety and attached CN and amine groups. However, in compounds **12s,t** and bithienoketone **15d**, the HOMO are delocalized over the entire molecule. Upon HOMO-LUMO excitation, a considerable transfer of electron density from the aryl substituent to the thiophene skeleton was observed. The LUMO densities were shifted onto the thiophenes and aromatic ring and CN, and the substituent on the amino group exhibit depleted electron density.

For internal use, please do not delete. Submitted_Manuscript

FULL PAPER

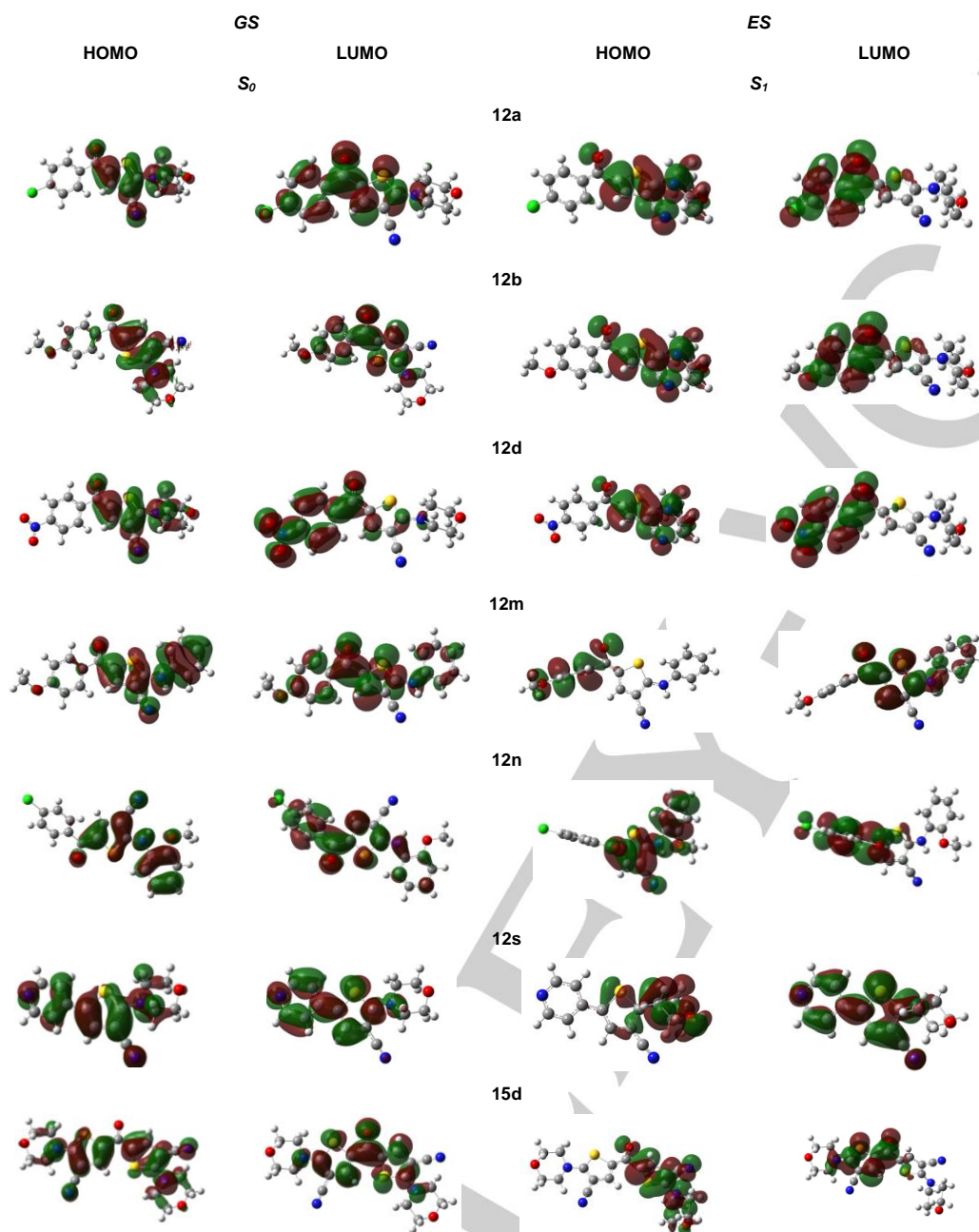


Figure 5. Frontier molecular orbitals (FMOs) HOMO and LUMO in ground and excited states for rotamers **B** of thiophenes **12a,b,d,m,n,s** and **15d** ($|\text{Isovalue}(\text{MO})| = 0.02$; $|\text{Isovalue}(\rho)| = 0.0004$).

According to the computed excited state optimized geometries, the presence of a twisted intramolecular charge transfer (TICT) exists where the two subunits that participate in the charge transfer process (the donor and acceptor of electron density) are orbitally decoupled. Emission from the TICT state to the ground state involves orbitals that are localized in different, spatially orthogonal π -systems. Therefore, their overlap is negligible, and this transition has a small transition moment and effectivity, which explains the origin of the low fluorescence quantum yield and the large

Stokes shift. The most remarkable geometrical change after TICT was observed for compound **12n**.

In bithienoketones **15**, the first absorption band was dominated by the HOMO \rightarrow LUMO transition. Therefore, analysis of the HOMO–LUMO overlap provides useful insight into the transition effectivity. The overlap between the HOMOs and LUMOs in the ground state is relatively large in all cases. In contrast, the overlap between the HOMOs and LUMOs in the excited state is smaller in all cases.

For internal use, please do not delete. Submitted_Manuscript

FULL PAPER

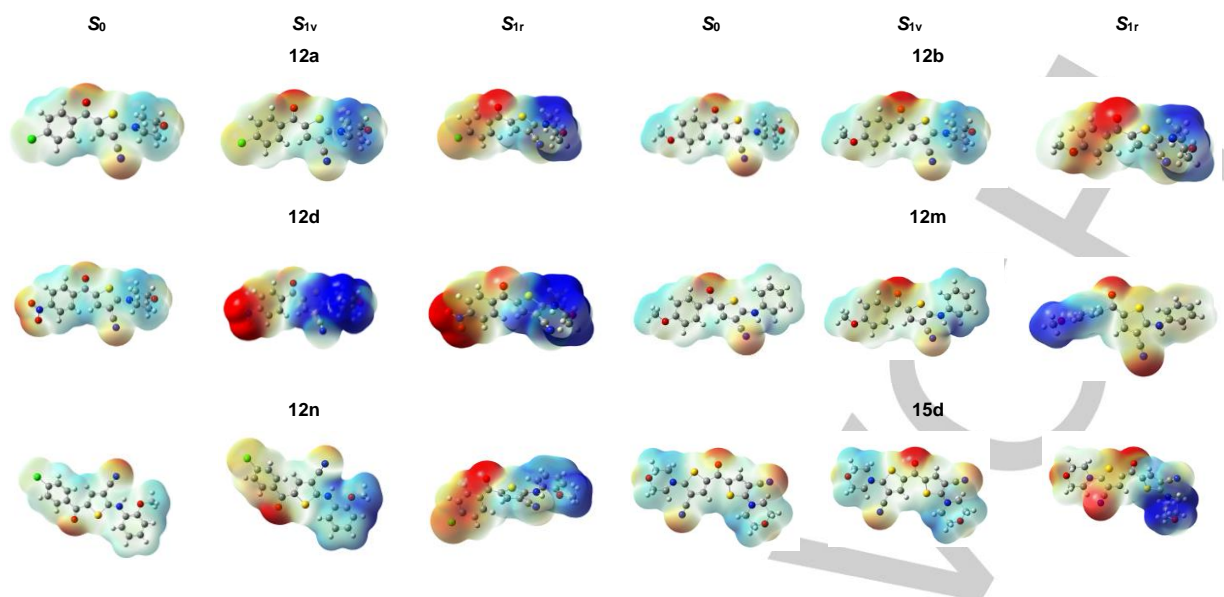


Figure 6. Molecular electric potential (MEP) calculated in solution (1,4-dioxane) for the most stable rotamer of thiophenes **12a, b, d, m, n** and **15d** in the ground and excited states. Legend of MEP colours: red (negative potential) and blue (positive potential). Legend of elements: hydrogen (white), carbon (grey), nitrogen (blue), and oxygen (red)..

Additional confirmation of the change in polarity and the ICT nature of the excited state comes from analysis of the MEP plots, which are shown in Figure 6 for several examples (additional examples are presented in the SI, Figure S42, 43). In their ground state, compounds **12a-d, i, l-n, s, t** and **15d** possess carbonyl and CN groups that are surrounded by a slightly negative electrostatic potential, and therefore, these groups may represent suitable sites for electrophilic attack. In contrast, a positive potential surrounds the amino group. Based on the MEP computed for the excited state (both after absorption and for the emissive minimum), these results confirm the increase in the charge separation after photon absorption and further increase after relaxation.

Conclusions

In this study, we developed an efficient, two-step alternative procedure for the synthesis of thiophenes with remarkable optical and fluorescence properties. The carbon atom of enamine group thioamides **11** was proven to be a better electrophilic centre than the carbon atom of the CN group. The heterocyclization results in the formation of a series of 5-acetyl-2-aminothiophenes. The proposed synthesis of trisubstituted thiophenes starts from simple initial compounds, such as 3-amino-2-cyanopropene thioamides, DMFDMA, and various halocarbonyl compounds, e.g., 2- and 4-picolyl chlorides. Trisubstituted thiophenes were produced in excellent yields. The current method is also promising due to its simple reaction

conditions, suggesting that this protocol may provide a valid alternative to previously reported protocols, which are tedious, time consuming, and result in poor yields using dangerous harsh conditions. Furthermore, the current protocol can be readily extended to the synthesis of libraries of new thiophene compounds incorporating various combinations of secondary or *tert*-cyclic amines as well as a range of halogen partners.

Another important result of this work is the photophysical properties of the newly synthesized mono- and bithienoketones. Most of these compounds exhibit fluorescence that is sensitive to the nature of the solvent polarity. Among the reported examples, the most efficient combinations of thiophene attached fragments is the anisoyl functionality at C5 thiophene and cycloalkylamine or phenylamine group at C2 thiophene. The experimental data and quantum chemical calculations revealed the presence of an ICT state during absorption that converts to a TICT state after geometry relaxation in the excited state. This behavior clarifies the origin of the remarkable fluorosolvatochromism of the new compounds. The TICT fluorescence has great promise in materials chemistry and life science research (i.e., biomedical imaging and diagnostics, in optoelectronic devices, and photovoltaic application).^[13a] Due to their photophysical properties and environmental sensitivity, these new compounds may find important applications in many fields, especially in biology, due to their structural similarity to biologically active thiophenes.

For internal use, please do not delete. Submitted_Manuscript

FULL PAPER

Experimental Section

General information and materials

All reactants were obtained from Acros Organics (Geel, Belgium) and used without further purification. The ^1H NMR and ^{13}C NMR spectra were recorded using a Bruker Avance II (Karlsruhe, Germany) (400 MHz for ^1H , 100 MHz for ^{13}C) spectrometer. The chemical shifts are reported in parts per million (ppm) relative to TMS for the ^1H NMR spectra and the residual solvent signals for the ^{13}C NMR spectra. The coupling constant (J) values are given in hertz (Hz). The signal splitting patterns are described as a singlet (s), doublet (d), triplet (t), quartet (q), sextet (sext), quintet (quin), multiplet (m), broad (br), doublet of doublets (dd), doublet of triplets (dt) or AA'XX' - spin system of para-substituted benzene with two different substituents. The major isomer signal is highlighted with an asterisk (*). The ^{13}C NMR signal patterns for several compounds were performed using the APT (attached proton test) and are described as follows: + for secondary or quaternary carbon atoms (positive signal) and - for primary or tertiary carbon atoms (negative signal). The mass spectra were recorded on a Shimadzu GCMS-QP 2010 "Ultra" (Kyoto, Japan) mass spectrometer using the electron impact (EI) ionization technique (40–200 °C, 70 eV). The $[M]^+$ abbreviation refers to the molecular ion. The IR spectra were obtained on an FTIR-ATR (attenuated total reflection, ZnSe) spectrometer (neat) in the 4000–400 cm^{-1} region (Ettlingen, Germany). Elemental analysis was conducted on a CHNS/O Perkin-Elmer 2400 Series II analyser instrument (Shelton, CT USA). The melting points were determined on a Stuart SMP3 apparatus (Staffordshire, ST15 OSA, UK). The reactions were monitored by analytical thin-layer chromatography (TLC) on aluminium-backed silica gel plates (Sorbfil UV–254). The components were visualized using a short wavelength UV light (254 nm). The solvents were dried and distilled according to common procedures. All solvents were of spectroscopic grade.

The title products were purified by column chromatography on silica gel (0.035–0.070, 60 Å) and recrystallized from ethanol.

Cyanothioacetamides (**5a–h**) and aminothioacrylamides (**9a–h** and **11a–c**) were prepared according to previously published procedures.^[9,10] Full experimental details for the synthesis of aminothioacrylamides (**9a–h** and **11a–c**), as well as the ^1H NMR and ^{13}C NMR spectra of new compounds **9a–h**, **11a–c**, **12a–t** and **15a–d**, photophysical characterization, and quantum mechanical calculation data are reported in the Supporting Information.

General procedure A to prepare compounds 12: Phenacyl bromides **2a–d** (1.2 mmol) were added to a solution of thioamides **9a–h** or **11a–d** (1.1 mmol) in DMF (4.0 ml). The mixture was maintained at 80 °C for 0.5–4.0 h, diluted with ethanol (10 ml) and maintained at 10–12 °C for 30 minutes. The precipitate was collected by filtration.

General procedure B to prepare compounds 12: Halomethylene compounds (1.2 mmol) **2e–j** and TEA (0.15 ml, 1.1 mmol) were added to the solution containing thioamides **9a,d,g** (1.1 mmol) in 4.0 ml of DMF. The mixture was maintained at 80 °C for 0.5–4.0 h. The solution was diluted with ethanol (10 ml) and maintained at 10–12 °C for 30 minutes. The precipitate was collected by filtration.

General procedure to prepare compounds 15: To the solution containing dichloroacetone **14** (0.26 g, 1.15 mmol), the solution containing propentioamides **9a–c** (0.25 g, 1.10 mmol) in DMF (3.0 ml) was added. The mixture was maintained at 80 °C for 0.5–2.0 h, diluted with ethanol (10 ml) and maintained at 10–12 °C for 30 minutes. The precipitate was collected by filtration.

5-(4-Chlorobenzoyl)-2-morpholinothiophene-3-carbonitrile (12a): Beige color powder (*method A*, 72 %); mp 175–177 °C; IR (ATR, ZnSe): $\nu = 3055, 3008, 2957, 2913, 2871, 2217, 1633 \text{ cm}^{-1}$; ^1H NMR (400 MHz, DMSO- d_6 , TMS): $\delta_{\text{H}} = 7.64$ (s, 1H, CH), 7.78 and 7.54 (AA'XX', 4H, $J = 8.4 \text{ Hz}$, H_{Ar}), 3.84–3.82 (m, 4H, 2CH₂), 3.71–3.69 ppm (m, 4H, 2CH₂); ^{13}C NMR (100 MHz, DMSO- d_6) $\delta_{\text{C}} = 184.4$ (+), 170.5 (+), 140.3 (-), 137.5 (+), 135.8 (+), 131.0 (2C) (-), 129.3 (2C) (-), 125.8 (+), 116.7 (+), 86.7 (+), 65.5 (2C) (+), 50.5 ppm (2C) (+); MS (EI) m/z (%): 332 (M^+ , 100); elemental analysis calcd (%) for C₁₆H₁₃ClN₂O₂S: C 57.74, H 3.94, N 8.42; found: C 57.5, H 4.2, N 8.1.

5-(4-Methoxybenzoyl)-2-morpholinothiophene-3-carbonitrile (12b): White crystals (*method A*, 93 %); mp 113–115 °C; IR (ATR, ZnSe): $\nu = 2971, 2913, 2878, 2843, 2208, 1624 \text{ cm}^{-1}$; ^1H NMR (400 MHz, DMSO- d_6 , TMS): $\delta_{\text{H}} = 7.58$ (s, 1H, CH), 7.77 and 7.03 (AA'XX', $J = 8.8 \text{ Hz}$, 4H, H_{Ar}), 3.89 (s, 3H, OMe), 3.84–3.81 (m, 4H, 2CH₂), 3.68–3.66 ppm (m, 4H, 2CH₂); ^{13}C NMR (100 MHz, DMSO- d_6) $\delta_{\text{C}} = 183.7, 169.6, 162.6, 138.2, 130.9$ (2C), 129.1, 126.3, 116.3, 114.0 (2C), 86.0, 65.0 (2C), 55.5, 50.0 ppm (2C); MS (EI) m/z (%): 328 (M^+ , 70); elemental analysis calcd (%) for C₁₇H₁₆N₂O₃S: C 62.18, H 4.91, N 8.53; found: C 61.9, H 5.0, N 8.3.

5-Benzoyl-2-morpholinothiophene-3-carbonitrile (12c): White crystals (*method A*, 62 %); mp 146–148 °C; IR (ATR, ZnSe): $\nu = 3101, 3054, 2991, 2947, 2868, 2215, 1625 \text{ cm}^{-1}$; ^1H NMR (400 MHz, DMSO- d_6 , TMS): $\delta_{\text{H}} = 7.79$ (d, $J = 7.4 \text{ Hz}$, 2H, H_{Ar}), 7.72 (s, 1H, CH), 7.65 (t, $J = 7.3 \text{ Hz}$, 1H, H_{Ar}), 7.55 (t, $J = 7.4 \text{ Hz}$, 2H, H_{Ar}), 3.81–3.78 (m, 4H, 2CH₂), 3.69–3.67 ppm (m, 4H, 2CH₂); ^{13}C NMR (100 MHz, DMSO- d_6) $\delta_{\text{C}} = 185.1, 169.9, 139.3, 136.7, 132.2, 128.7$ (2C), 128.6 (2C), 125.8, 116.2, 86.2, 65.0 (2C), 50.1 ppm (2C); MS (EI) m/z (%): 298 (M^+ , 91); elemental analysis calcd (%) for C₁₆H₁₄N₂O₂S: C 64.41, H 4.73, N 9.39; found: C 64.2, H 5.0, N 9.2.

2-Morpholino-5-(4-nitrobenzoyl)thiophene-3-carbonitrile (12d): Bright-yellow crystals (*method A*, 63 %); mp 197–199 °C; IR (ATR, ZnSe): $\nu = 3104, 3091, 3043, 2993, 2877, 2210, 1628 \text{ cm}^{-1}$; ^1H NMR (400 MHz, DMSO- d_6 , TMS): $\delta_{\text{H}} = 8.35$ and 7.99 (AA'XX', $J = 8.7 \text{ Hz}$, 4H, H_{Ar}), 7.72 (s, 1H, CH), 3.84–3.81 (m, 4H, 2CH₂), 3.74–3.71 ppm (m, 4H, 2CH₂); ^{13}C NMR (100 MHz, DMSO- d_6) $\delta_{\text{C}} = 183.6$ (+), 170.3 (+), 149.2 (+), 142.0 (-), 129.9 (2C) (-), 124.8 (+), 123.8 (2C) (-), 116.1 (+), 86.4 (+), 65.0 (2C) (+), 50.2 ppm (2C) (+); MS (EI) m/z (%): 343 (M^+ , 100); elemental analysis calcd (%) for C₁₆H₁₃N₃O₄S: C 55.97, H 3.82, N 12.24; found: C 55.7, H 4.0, N 11.9.

5-(4-Methoxybenzoyl)-2-(piperidin-1-yl)thiophene-3-carbonitrile (12e): White powder (*method A*, 90 %); mp 108–109 °C; IR (ATR, ZnSe): $\nu = 2951, 2923, 2844, 2206, 1628 \text{ cm}^{-1}$; ^1H NMR (400 MHz, DMSO- d_6 , TMS): $\delta_{\text{H}} = 7.50$ (s, 1H, CH), 7.75 and 7.01 (AA'XX', $J = 8.8 \text{ Hz}$, 4H, H_{Ar}), 3.89 ppm (s, 3H, OMe), 3.73–3.71 (m, 4H, 2CH₂), 1.78–1.76 (m, 6H, 3CH₂); ^{13}C NMR (100 MHz, DMSO- d_6) $\delta_{\text{C}} = 183.6$ (+), 169.0 (+), 162.4 (+), 138.6 (-), 130.8 (2C) (-), 129.2 (+), 125.2 (+), 116.5 (+), 113.9 (2C) (-), 85.1 (+), 55.5 (-), 51.8 (2C) (+), 24.7 (2C) (+), 22.8 (+) ppm; MS (EI) m/z (%): 326 (M^+ , 100); elemental analysis calcd (%) for C₁₈H₁₈N₂O₂S: C 66.23, H 5.56, N 8.58; found: C 65.9, H 5.7, N 8.3.

5-(4-Methoxybenzoyl)-2-(pyrrolidin-1-yl)thiophene-3-carbonitrile (12f): Beige color powder (*method A*, 80 %); mp 135–136 °C; IR (ATR, ZnSe): $\nu = 2979, 2956, 2849, 2210, 1620 \text{ cm}^{-1}$; ^1H NMR (400 MHz, DMSO- d_6 , TMS): $\delta_{\text{H}} = 7.50$ (c, 1H, CH), 7.73 and 7.00 (AA'XX', $J = 8.8 \text{ Hz}$, 4H, H_{Ar}), 3.88 (s, 3H, OMe), 3.71–3.67 (m, 4H, 2CH₂), 2.16–2.12 ppm (m, 4H, 2CH₂); ^{13}C NMR (100 MHz, DMSO- d_6) $\delta_{\text{C}} = 183.4$ (+), 165.3 (+), 162.4 (+), 138.4 (-), 130.7 (2C) (-), 129.5 (+), 124.0 (+), 116.9 (+), 113.9 (2C) (-), 83.5 (+), 55.4 (-), 51.9 (2C) (+), 25.4 ppm (2C) (+); MS (EI) m/z (%): 312 (M^+ , 100); elemental analysis calcd (%) for C₁₇H₁₆N₂O₂S: C 65.36, H 5.16, N 8.97; found: C 65.1, H 5.3, N 8.7.

5-(4-Chlorobenzoyl)-2-(pyrrolidin-1-yl)thiophene-3-carbonitrile (12g): Beige color powder (*method A*, 67 %); mp 190–191 °C; IR (ATR, ZnSe): $\nu = 3096, 3058, 2961, 2867, 2209, 1618 \text{ cm}^{-1}$; ^1H NMR (400 MHz, DMSO- d_6 , TMS): $\delta_{\text{H}} = 7.58$ (s, 1H, CH), 7.75 and 7.52 (AA'XX', $J = 8.5 \text{ Hz}$, 4H, H_{Ar}), 3.71–3.67 (m, 4H, 2CH₂), 2.15–2.12 ppm (m, 4H, 2CH₂); ^{13}C NMR (100 MHz, DMSO- d_6) $\delta_{\text{C}} = 183.9$ (+), 166.4 (+), 140.1 (-), 137.2 (+), 136.4 (+), 130.7 (2C) (-), 129.1 (2C) (-), 124.7 (+), 117.0 (+), 84.7 (+), 52.6 (2C)

For internal use, please do not delete. Submitted Manuscript

FULL PAPER

(+), 25.8 ppm (2C) (+); MS (EI) m/z (%): 316 (M^+ , 100); elemental analysis calcd (%) for $C_{16}H_{13}ClN_2OS$: C 60.66, H 4.14, N 8.84; found: C 60.3, H 4.3, N 8.6.

5-(4-Methoxybenzoyl)-2-(methylamino)thiophene-3-carbonitrile

(11h): White crystals (*method A*, 87 %); mp 236-237 °C; IR (ATR, ZnSe): $\nu = 3289, 2916, 2885, 2212, 1615 \text{ cm}^{-1}$; $^1\text{H NMR}$ (400 MHz, DMSO- d_6 , TMS): $\delta_{\text{H}} = 8.60$ (q, 1H, $J = 4.7 \text{ Hz}$, NH), 7.72 and 6.99 (AA'XX', $J = 8.7 \text{ Hz}$, 4H, H_{Ar}), 7.71 (s, 1H, CH), 3.88 (s, 3H, OMe), 2.99 ppm (d, 3H, $J = 4.7 \text{ Hz}$, NMe); $^{13}\text{C NMR}$ (100 MHz, DMSO- d_6) $\delta_{\text{C}} = 183.5$ (+), 171.0 (+), 162.3 (+), 137.4 (-), 130.6 (2C) (-), 129.6 (+), 124.4 (+), 115.1 (+), 113.9 (2C) (-), 84.2 (+), 55.4 (-), 33.8 ppm (-); MS (EI) m/z (%): 272 (M^+ , 58); elemental analysis calcd (%) for $C_{14}H_{12}N_2O_2S$: C 61.75, H 4.44, N 10.29; found: C 61.5, H 4.6, N 10.0.

5-(4-Chlorobenzoyl)-2-(methylamino)thiophene-3-carbonitrile (12i)

Beige color powder (*method A*, 62 %); mp 281-283 °C; IR (ATR, ZnSe): $\nu = 3309, 3088, 2926, 2211, 1613 \text{ cm}^{-1}$; $^1\text{H NMR}$ (400 MHz, DMSO- d_6 , TMS): $\delta_{\text{H}} = 8.75$ (br s, 1H, NH), 7.55 (s, 1H, CH), 7.74 and 7.51 (AA'XX', $J = 8.5 \text{ Hz}$, 4H, H_{Ar}), 3.00 ppm (d, $J = 4.7 \text{ Hz}$, 3H, NHMe); $^{13}\text{C NMR}$ (100 MHz, DMSO- d_6) $\delta_{\text{C}} = 184.0$ (+), 172.0 (+), 139.6 (-), 137.1(+), 136.3(+), 130.8 (2C) (-), 129.9 (2C) (-), 124.0 (+), 115.5 (+), 85.2 (+), 34.4 ppm (-); MS (EI) m/z (%): 276 (M^+ , 91); elemental analysis calcd (%) for $C_{13}H_9ClN_2OS$: C 56.42, H 3.28, N 10.12; found: C 56.2, H 3.5, N 9.9.

2-(Butylamino)-5-(4-chlorobenzoyl)thiophene-3-carbonitrile (12j)

Light-brown powder (*method A*, 72 %); mp 157-159 °C; IR (ATR, ZnSe): $\nu = 3271, 3097, 2961, 2936, 2867, 2210, 1614 \text{ cm}^{-1}$; $^1\text{H NMR}$ (400 MHz, DMSO- d_6 , TMS): $\delta_{\text{H}} = 8.92$ (br s, 1H, NH), 7.68 (s, 1H, CH), 7.77 и 7.58 (AA'XX', $J = 8.0 \text{ Hz}$, 4H, H_{Ar}), 3.28 (q, $J = 6.5 \text{ Hz}$, 2H, CH₂NH), 1.64 (sext, $J = 7.4 \text{ Hz}$, 2H, CH₂), 1.37 (quin, $J = 7.3 \text{ Hz}$, 2H, CH₂), 0.93 ppm (t, $J = 7.4 \text{ Hz}$, 3H, Me); $^{13}\text{C NMR}$ (100 MHz, DMSO- d_6) $\delta_{\text{C}} = 183.5, 170.4, 139.1, 136.6, 135.8, 130.3$ (2C), 128.7 (2C), 123.2, 115.1, 84.8, 47.6, 29.7, 19.4, 13.5 ppm; MS (EI) m/z (%): 318 (M^+ , 65); elemental analysis calcd (%) for $C_{16}H_{15}ClN_2OS$: C 60.28, H 4.74, N 8.79; found: C 59.9, H 4.9, N 8.6.

2-(Benzylamino)-5-(4-chlorobenzoyl)thiophene-3-carbonitrile (12k)

Lemon color powder (*method A*, 93 %); mp 279-281 °C; IR (ATR, ZnSe): $\nu = 3234, 3097, 3060, 3029, 3001, 2214, 1613 \text{ cm}^{-1}$; $^1\text{H NMR}$ (400 MHz, DMSO- d_6 , TMS): $\delta_{\text{H}} = 9.39$ (t, 1H, $J = 5.8 \text{ Hz}$, NH), 7.53 (s, 1H, CH), 7.72 и 7.50 (AA'XX', $J = 8.4 \text{ Hz}$, 4H, H_{Ar}), 7.42-7.34 (m, 4H, H_{Ar}), 7.31-7.27 (m, 1H, H_{Ar}), 4.50 ppm (d, $J = 5.9 \text{ Hz}$, 2H, CH₂); $^{13}\text{C NMR}$ (100 MHz, DMSO- d_6) $\delta_{\text{C}} = 183.6, 170.3, 138.7, 136.6, 136.3, 135.7, 130.3$ (2C), 128.7 (2C), 128.6 (2C), 127.7 (2C), 124.0, 114.9, 85.6, 50.6 ppm; MS (EI) m/z (%): 352 (M^+ , 6); elemental analysis calcd (%) for $C_{19}H_{13}ClN_2OS$: C 64.68, H 3.71, N 7.94; found: C 64.4, H 3.9, N 7.6.

5-(4-Chlorobenzoyl)-2-(phenylamino)thiophene-3-carbonitrile (12l)

Sand color powder (*method A*, 96 %); mp 195-197 °C; IR (ATR, ZnSe): $\nu = 3261, 3095, 3062, 3022, 2980, 2218, 1614 \text{ cm}^{-1}$; $^1\text{H NMR}$ (400 MHz, DMSO- d_6 , TMS): $\delta_{\text{H}} = 10.55$ (s, 1H, NH), 7.78 и 7.54 (AA'XX', $J = 8.4 \text{ Hz}$, 4H, H_{Ar}), 7.67 (s, 1H, CH), 7.41-7.47 (m, 4H, H_{Ar}), 7.22 ppm (t, 1H, $J = 4.6 \text{ Hz}$, H_{Ar}); $^{13}\text{C NMR}$ (100 MHz, DMSO- d_6) $\delta_{\text{C}} = 184.1, 166.3, 140.3, 138.0, 137.0, 135.5, 130.5$ (2C), 129.7 (2C), 128.8 (2C), 125.5, 124.9, 121.1 (2C), 114.5, 89.7 ppm; MS (EI) m/z (%): 338 (M^+ , 100); elemental analysis calcd (%) for $C_{18}H_{11}ClN_2OS$: C 63.81, H 3.27, N 8.27; found: C 63.6, H 3.5, N 8.0.

5-(4-Methoxybenzoyl)-2-(phenylamino)thiophene-3-carbonitrile

(12m): Sand color powder (*method A*, 72 %); mp 194-196 °C; IR (ATR, ZnSe): $\nu = 3278, 3149, 3095, 3069, 3026, 2980, 2919, 2828, 2216, 1600 \text{ cm}^{-1}$; $^1\text{H NMR}$ (400 MHz, DMSO- d_6 , TMS): $\delta_{\text{H}} = 10.39$ (s, 1H, NH), 7.77 (d, $J = 8.8 \text{ Hz}$, 2H, H_{Ar}), 7.59 (s, 1H, CH), 7.46-7.41 (m, 4H, H_{Ar}), 7.17 (t, $J = 7.0 \text{ Hz}$, 1H, H_{Ar}), 7.02 (d, $J = 8.8 \text{ Hz}$, 2H, H_{Ar}), 3.89 ppm (s, 3H, OMe); $^{13}\text{C NMR}$ (100 MHz, DMSO- d_6) $\delta_{\text{C}} = 184.5$ (+), 166.0 (+), 163.1 (+), 141.0 (+), 136.9 (-), 131.4 (2C) (-), 130.1 (2C) (-), 129.8 (+), 126.4 (+), 125.7 (-), 121.3 (2C) (-), 115.1 (+), 114.5 (2C) (-), 90.1 (+), 56.0 ppm (-); MS (EI) m/z (%): 334 (M^+ , 63); elemental analysis calcd (%) for $C_{19}H_{14}N_2O_2S$: C 68.25, H 4.22, N 8.38; found: C 68.0, H 4.4, N 8.1.

5-(4-Chlorobenzoyl)-2-((2-methoxyphenyl)amino)thiophene-3-carbonitrile (12n)

Bright-yellow crystals (*method A*, 84 %); mp 226-

228 °C; IR (ATR, ZnSe): $\nu = 3350, 3094, 3063, 3025, 2953, 2211, 1624 \text{ cm}^{-1}$; $^1\text{H NMR}$ (400 MHz, DMSO- d_6 , TMS): $\delta_{\text{H}} = 10.00$ (s, 1H, NH), 7.58 (s, 1H, CH), 7.75 и 7.52 (AA'XX', $J = 7.6 \text{ Hz}$, 4H, H_{Ar}), 7.34-7.30 (m, 2H, H_{Ar}), 7.14 (d, $J = 7.9 \text{ Hz}$, 1H, H_{Ar}), 7.02 (t, $J = 7.0 \text{ Hz}$, 1H, H_{Ar}), 3.89 ppm (s, 3H, OMe); $^{13}\text{C NMR}$ (100 MHz, DMSO- d_6) $\delta_{\text{C}} = 183.8$ (+), 169.0 (+), 153.3 (+), 138.2 (-), 136.7 (+), 135.6 (+), 130.3 (2C) (-), 128.6 (2C) (-), 128.5 (-), 128.1 (+), 125.8 (-), 124.9 (+), 120.8 (-), 114.4 (+), 112.6 (-), 87.4 (+), 55.6 ppm (-); MS (EI) m/z (%): 369 (M^+ , 68); elemental analysis calcd (%) for $C_{19}H_{13}ClN_2O_2S$: C 61.87, H 3.55, N 7.60; found: C 61.5, H 3.8, N 7.3.

5-Acetyl-2-morpholinothiophene-3-carbonitrile (12o)

Beige crystals (*method B*, 78 %); mp 207-209 °C; IR (ATR, ZnSe): $\nu = 3059, 2953, 2928, 2907, 2874, 2208, 1642 \text{ cm}^{-1}$; $^1\text{H NMR}$ (400 MHz, DMSO- d_6 , TMS): $\delta_{\text{H}} = 7.91$ (s, 1H, CH), 3.79-3.82 (m, 4H, 2CH₂), 3.61-3.63 (m, 4H, 2CH₂), 2.40 ppm (s, 3H, Me); $^{13}\text{C NMR}$ (100 MHz, DMSO- d_6) $\delta_{\text{C}} = 189.4$ (+), 170.3 (+), 138.3 (-), 127.6 (+), 116.8 (+), 85.9 (+), 65.5 (2C) (+), 50.5 (2C) (+), 25.5 ppm (-); MS (EI) m/z (%): 236 (M^+ , 100); elemental analysis calcd (%) for $C_{11}H_{12}N_2O_2S$: C 55.92, H 5.12, N 11.86; found: C 55.7, H 5.3, N 11.6.

Ethyl 4-cyano-5-morpholinothiophene-2-carboxylate (12p)

Beige crystals (*method B*, 56 %); mp 136-138 °C; IR (ATR, ZnSe): $\nu = 3107, 3063, 2992, 2973, 2930, 2907, 2878, 2210, 1696 \text{ cm}^{-1}$; $^1\text{H NMR}$ (400 MHz, DMSO- d_6 , TMS): $\delta_{\text{H}} = 7.64$ (s, 1H, CH); 4.25 (q, 2H, $J = 7.1 \text{ Hz}$, CH₂CH₃), 3.82-3.79 (m, 4H, 2CH₂), 3.59-3.57 (m, 4H, 2CH₂), 1.32 ppm (t, $J = 7.1 \text{ Hz}$, 3H, CH₃); $^{13}\text{C NMR}$ (100 MHz, DMSO- d_6) $\delta_{\text{C}} = 169.5$ (+), 160.9 (+), 136.9 (-), 116.5 (+), 116.0 (+), 86.5 (+), 65.5 (2C) (+), 61.4 (+), 50.6 (2C) (+), 14.6 ppm (-); MS (EI) m/z (%): 266 (M^+ , 100); elemental analysis calcd (%) for $C_{12}H_{14}N_2O_3S$: C 54.12, H 5.30, N 10.52; found: C 53.9, H 5.5, N 10.3.

Ethyl 2-(4-cyano-5-morpholinothiophen-2-yl)-2-oxoacetate (12q)

Yellow crystals (*method B*, 84 %); mp 131-132 °C; IR (ATR, ZnSe): $\nu = 3105, 2978, 2907, 2873, 2211, 1738, 1642 \text{ cm}^{-1}$; $^1\text{H NMR}$ (400 MHz, DMSO- d_6 , TMS): $\delta_{\text{H}} = 8.18$ (s, 1H, CH), 4.34 (q, $J = 7.1 \text{ Hz}$, 2H, CH₂CH₃), 3.80-3.72 (m, 8H, 4CH₂), 1.32 ppm (t, $J = 7.1 \text{ Hz}$, 3H, CH₃); $^{13}\text{C NMR}$ (100 MHz, DMSO- d_6) $\delta_{\text{C}} = 173.9, 170.4, 161.3, 142.9, 121.2, 115.9, 86.7, 65.0$ (2C), 62.4, 50.3 (2C), 13.8 ppm; MS (EI) m/z (%): 294 (M^+ , 100); elemental analysis calcd (%) for $C_{13}H_{14}N_2O_4S$: C 53.05, H 4.79, N 9.52; found: C 52.8 H 4.9, N 9.6.

5-Morpholinothiophene-2,4-dicarbonitrile (12r)

Beige color powder (*method B*, 83 %); mp 150-152 °C; IR (ATR, ZnSe): $\nu = 2921, 2852, 2201, 1635 \text{ cm}^{-1}$; $^1\text{H NMR}$ (400 MHz, DMSO- d_6 , TMS): $\delta_{\text{H}} = 7.88$ (s, 1H, CH), 3.79-3.82 (m, 4H, 2CH₂), 3.58-3.61 ppm (m, 4H, 2CH₂); $^{13}\text{C NMR}$ (100 MHz, DMSO- d_6) $\delta_{\text{C}} = 169.1$ (+), 142.7 (-), 116.1 (+), 114.4 (+), 91.7 (+), 85.7 (+), 65.4 (2C) (+), 50.7 ppm (2C) (+); MS (EI) m/z (%): 219 (M^+ , 100); elemental analysis calcd (%) for $C_{10}H_9N_3OS$: C 54.78, H 4.14, N 19.16; found: C 54.6, H 3.9, N 18.8.

2-Morpholino-5-(pyridin-4-yl)thiophene-3-carbonitrile (12s)

Pale-yellow powder (*method B*, 92 %); mp 117-119 °C; IR (ATR, ZnSe): $\nu = 3054, 2957, 2867, 2202, 1598 \text{ cm}^{-1}$; $^1\text{H NMR}$ (400 MHz, DMSO- d_6 , TMS): $\delta_{\text{H}} = 8.48$ (br s, 2H, H_{Ar}), 7.71 (s, 1H, CH), 7.41 (d, $J = 5.0 \text{ Hz}$, 2H, H_{Ar}), 3.84-3.82 (m, 4H, 2CH₂), 3.55-3.52 ppm (m, 4H, 2CH₂); $^{13}\text{C NMR}$ (100 MHz, DMSO- d_6) $\delta_{\text{C}} = 166.5, 150.2, 139.4, 127.8$ (2C), 124.0, 118.3 (2C), 116.4, 87.1, 65.1 (2C), 50.5 ppm (2C); MS (EI) m/z (%): 271 (M^+ , 100); elemental analysis calcd (%) for $C_{14}H_{13}N_3OS$: C 61.97, H 4.83, N 15.49; found: C 61.7, H 5.0, N 15.1.

2-Morpholino-5-(pyridin-2-yl)thiophene-3-carbonitrile (12t)

White crystals (*method B*, 93 %); mp 157-159 °C; IR (ATR, ZnSe): $\nu = 3064, 3000, 2928, 2872, 2206, 1585 \text{ cm}^{-1}$; $^1\text{H NMR}$ (400 MHz, DMSO- d_6 , TMS): $\delta_{\text{H}} = 8.40$ (d, $J = 4.7 \text{ Hz}$, 1H, H_{Ar}), 7.71-7.79 (m, 2H, H_{Ar}), 7.67 (s, 1H, CH), 7.18-7.15 (m, 1H, H_{Ar}), 3.81-3.83 (m, 4H, 2CH₂), 3.52-3.54 ppm (m, 4H, 2CH₂); $^{13}\text{C NMR}$ (100 MHz, DMSO- d_6) $\delta_{\text{C}} = 167.2$ (+), 150.8 (+), 149.2 (-), 136.9 (-), 128.9 (+), 126.1 (-), 121.8 (-), 117.6 (-), 116.9 (+), 86.5 (+), 65.2 (2C) (+), 50.2 ppm (2C) (+); MS (EI) m/z (%): 271 (M^+ , 100); elemental analysis calcd (%) for $C_{14}H_{13}N_3OS$: C 61.97, H 4.83, N 15.49; found: C 61.6, H 4.9, N 15.3.

5,5'-Carbonylbis(2-(methylamino)thiophene-3-carbonitrile) (15a)

Orange color powder (60 %); mp 326-327 °C; IR (ATR, ZnSe): $\nu = 3336, 3259, 3093, 2973, 2948, 2901, 2214, 1582 \text{ cm}^{-1}$; $^1\text{H NMR}$ (400 MHz,

For internal use, please do not delete. Submitted Manuscript

FULL PAPER

DMSO-*d*₆, TMS): $\delta_{\text{H}} = 8.63$ (d, $J = 4.7$ Hz, 2H, 2NH), 8.11 (s, 2H, 2CH), 2.92 ppm (d, 6H, $J = 4.7$ Hz, 2CH₃); ¹³C NMR (100 MHz, DMSO-*d*₆) $\delta_{\text{C}} = 173.8$ (+), 170.7 (2C) (+), 135.5 (2C) (-), 123.4 (2C) (+), 115.8 (2C) (+), 84.7 (2C) (+); 34.2 ppm (2C) (-); MS (EI) m/z (%): 302 (M⁺, 100); elemental analysis calcd (%) for C₁₉H₁₄ClN₃O₃S: C 51.64, H 3.33, N 18.53; found: C 51.3, H 3.5, N 18.3.

5,5'-Carbonylbis(2-(phenylamino)thiophene-3-carbonitrile) (15b): Brown crystals (93 %); mp 282-283 °C; ¹H NMR (400 MHz, DMSO-*d*₆, TMS): $\delta_{\text{H}} = 10.52$ (s, 2H, 2NH), 8.27 (s, 2H, 2CH); 7.44 (d, $J = 4.3$ Hz, 8H, 8CH_A); 7.21 ppm (quin, $J = 4.2$ Hz, 2H, 2CH_A); ¹³C NMR (100 MHz, DMSO-*d*₆) $\delta_{\text{C}} = 174.0$, 164.9 (2C), 155.8 (2C), 140.6 (2C), 134.9 (2C), 129.6 (4C), 125.1 (2C), 120.8 (4C), 114.8 (2C), 90.0 ppm (2C); MS (EI) m/z (%): 426 (M⁺, 100); elemental analysis calcd (%) for C₂₃H₁₄N₄O₂S: C 64.77, H 3.31, N 13.14; found: C 64.4, H 3.5, N 12.9.

5,5'-Carbonylbis(2-(pyrrolidin-1-yl)thiophene-3-carbonitrile) (15c): Yellow powder (77 %); mp 323-324 °C; IR (ATR, ZnSe): $\nu = 3071$, 2955, 2876, 2202, 1557 cm⁻¹; ¹H NMR (400 MHz, DMSO-*d*₆, TMS): $\delta_{\text{H}} = 8.32$ (s, 2H, 2CH), 3.62-3.65 (m, 8H, 4CH₂), 2.04-2.10 ppm (m, 8H, 4CH₂); ¹³C NMR (100 MHz, DMSO-*d*₆) $\delta_{\text{C}} = 168.8$, 158.2 (2C), 136.5 (2C), 123.5 (2C), 116.6 (2C), 83.9 (2C), 51.9 (4C), 25.3 ppm (4C); MS (EI) m/z (%): 382 (M⁺, 100); elemental analysis calcd (%) for C₁₉H₁₈N₄O₂S: C 59.66, H 4.74, N 14.65; found: C 59.4, H 4.9, N 14.3.

5,5'-Carbonylbis(2-morpholinothiophene-3-carbonitrile) (15d): Bright yellow powder (76 %); mp 320-321 °C; IR (ATR, ZnSe): $\nu = 3056$, 2955, 2912, 2873, 2214, 1602 cm⁻¹; ¹H NMR (400 MHz, DMSO-*d*₆, TMS): $\delta_{\text{H}} = 8.19$ (s, 2H, 2CH), 3.79-3.85 (m, 8H, 4CH₂), 3.61-3.67 ppm (m, 8H, 4CH₂); ¹³C NMR (100 MHz, DMSO-*d*₆) $\delta_{\text{C}} = 169.9$, 162.7 (2C), 136.9 (2C), 125.3 (2C), 116.7 (2C), 87.2 (2C), 65.6 (4C), 50.8 ppm (4C); MS (EI) m/z (%): 414 (M⁺, 100); elemental analysis calcd (%) for C₁₉H₁₈N₄O₃S₂: C 55.06, H 4.38, N 13.52; found: C 54.8, H 4.5, N 13.2.

5,5'-Carbonylbis(2-(piperidin-1-yl)thiophene-3-carbonitrile) (15e): Sand color powder (75 %); mp 315-316 °C. IR (ATR, ZnSe): $\nu = 2938$, 2922, 2854, 2205, 1559 cm⁻¹; ¹H NMR (400 MHz, DMSO-*d*₆, TMS): $\delta_{\text{H}} = 7.71$ (s, 2H, CH), 3.82-3.84 (m, 4H, 2CH₂), 3.52-3.55 ppm (m, 12H, 6CH₂); ¹³C NMR (100 MHz, DMSO-*d*₆) $\delta_{\text{C}} = 168.7$ (+), 157.0 (2C) (+), 136.5 (2C) (-), 123.8 (2C) (+), 116.4 (2C) (+), 85.7 (2C) (+), 51.9 (4C) (+), 24.7 (4C) (+), 22.7 ppm (2C) (+); MS (EI) m/z (%): 410 (M⁺, 100); elemental analysis calcd (%) for C₂₁H₂₂N₄O₂S: C 61.44, H 5.40, N 13.65; found: C 61.2, H 5.6, N 13.3.

Electronic absorption and emission spectroscopy

The UV-Vis absorption spectra were recorded on a Perkin-Elmer Lambda 35 UV-Vis spectrophotometer (Shelton, CT USA). The fluorescence of the sample solutions was measured using a Hitachi F-7000 spectrophotometer (Tokyo, Japan). The absorption and emission spectra were recorded in hexane, 1,4-dioxane, toluene, acetone, MeCN, THF, AcOEt, DCM, CH₂Cl₂, DMF, DMSO, *i*PrOH, and EtOH using 10.00 mm quartz cells. The excitation wavelength was equal to the absorption maxima. The atmospheric oxygen that was contained in the solutions was not removed. The concentrations of the compounds in the solution was 10⁻⁵ M and 10⁻⁶ M for the absorption and fluorescence measurements, respectively. The relative fluorescence quantum yields (Φ_{F}) were determined using quinine sulfate (10⁻⁵ M) in 0.1 M H₂SO₄ as a standard ($\Phi_{\text{F}} = 0.546$) or anthracene as a standard.^[14]

Quantum mechanical calculations

The ground state molecular geometry of all possible rotamers of the studied compounds was fully optimized using density functional theory (DFT) both in vacuum and in solvent (1,4-dioxane for all compounds; DCM, acetone, acetonitrile, and DMSO for a sub-set of the compounds, vide infra). We have compared the results obtained using different functionals

and different basis sets.^[16] In particular, we chose hybrid (viz. B3LYP,^[16a] and M06-2X^[16b]) and long-range corrected (viz. CAM-B3LYP^[16c] and ω B97X^[16d]) functionals coupled with the 6-31+G**, 6-311++G**, aug-cc-pVDZ and aug-cc-pVTZ^[17] basis sets. The D3 version of Grimme's semi-empirical dispersion with Becke-Johnson damping GD3BJ^[17f] was also included for the B3LYP, CAM-B3LYP, and ω B97X functionals. The solvent effects were taken into account using the implicit polarizable continuum model in its integral equation formalism (IEF-PCM).^[18] For geometry optimizations and frequency calculations, the PCM molecular cavity was constructed according to the universal force field (UFF)^[19] radii within the value used in the last implementation of the PCM (based on a continuum surface charge formalism). For topological analysis and evaluation of the energetics, SMD parameterization was employed.^[20] The standard values for the dielectric constants and refractive indices were always assumed. The vibrational frequencies and thermochemical values were computed with the harmonic approximation at T = 298.15 K and p = 1 atm, and no imaginary frequencies were found.

The UV-Vis absorption spectra for the equilibrium geometries of the ligand were calculated using time-dependent density functional theory (TD-DFT) accounting for S₀ → S_n (n = 1 to 5). The energy of the first 5 triplet states was also computed. The nature of the vertical excited electronic state was analysed both in vacuum and in the solvated phase. This investigation was performed by employing a long-range corrected functional (CAM-B3LYP) coupled with the 6-31+G** basis sets. For the solvated phase, state-specific (SS)^[21] treatment of the solvent effects was considered within both the non-equilibrium (neq) and equilibrium (eq) solvation regimes.^[22] In addition, the vibronic progressions^[23] of the S₀ → S₁ electronic transition were simulated including Duschinsky and Herzberg-Teller effects. The first singlet excited state (S(π,π*)) geometry was optimized using analytical gradients and the first transitions (S₁ → S₀) of the emission transition. In this case, SS (both eq and neq) treatment of the solvent effects was considered, and the electronic emission band was simulated by accounting for the vibronic progressions, as performed for absorption.

The atomic charge population analysis, electric multiple moments, electronic density, and electrostatic potential were also computed within the Mulliken and CHelpG procedure^[24] for both the ground and S₁ excited (vertical and relaxed) states.

To investigate the presence and nature of the possible intramolecular hydrogen bonding interactions, the non-covalent interaction (NCI) index combined with the second derivative of the reduced density gradient and the second main axis of variation were employed.^[12] These procedures were applied both to the ground and first singlet excited states.

For the topological and RDG analyses, the integration grid for the electronic density was set to 150 radial shells and 974 angular points. For the other calculations, the integration grid was set to 99 radial shells and 590 angular points. The convergence criteria for the self-consistent field were set to 10⁻¹² for the RMS change in the density matrix and 10⁻¹⁰ for the maximum change in the density matrix. The convergence criteria for optimizations were set to 2 × 10⁻⁶ a.u. for the maximum force, 1 × 10⁻⁶ a.u. for the RMS force, 6 × 10⁻⁶ a.u. for the maximum displacement and 4 × 10⁻⁶ a.u. for the RMS displacement.

All calculations were performed using the GAUSSIAN G09.D01 package.^[25] The location of the BCPs and subsequent calculation of the SF values were performed using a modified version of the PROAIMV program.^[26] The calculation of the RDG and its derivatives were performed using homemade codes.

Acknowledgements

The Government of the Russian Federation (Act 211, contract #02.A03.21.0006) supported the research. K. L. Thanks RFBR for

For internal use, please do not delete. Submitted_Manuscript

FULL PAPER

funding № 16-33-00327 mol_a. E. B. thanks the Italian “Ministero per l’Università e la Ricerca Scientifica e Tecnologica” for fundings [FIRB 2013, RBFR13PSB6].

Keywords: thiophene • fluorescence • solvatochromism • ICT • TICT

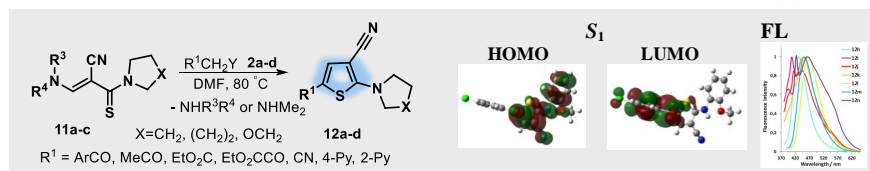
- [1] R. K. Russel, J. B. Press in *Comprehensive Heterocyclic Chemistry II* (Ed.: C. W. Bird), Elsevier, Amsterdam, **2005**, pp. 679-729.
- [2] a) M. A. Metwally, B. F. Abdel-Wahab, M. Koketsu, *Phosphorus, Sulfur, Silicon Relat. Elem.* **2009**, *184*, 3038–3074; b) R. M. Mohareb, A. E. M. Abdallah, M. A. Abdelaziz, *Med. Chem. Res.* **2014**, *23*, 564–579.
- [3] a) M. E. Cinar, T. Ozturk, *Chem. Rev.* **2015**, *115*, 3036–3140; b) M. S. M. Li, K. Chu, J. T. Price, N. D. Jones, Zh. Ding, *ChemElectroChem*, **2016**, *3*, 2170 – 2178.
- [4] a) B. S. Ong, Y. Wu, Y. Li, P. Liu, H. Pan, *Chem. Eur. J.* **2008**, *14*, 4766–4778; b) I. Osaka, R. D. McCullough, *Acc. Chem. Res.* **2008**, *41*, 1202–1214. c) S. Liu, Z. Kan, S. Thomas, F. Cruciani, J.-L. Bredas, P. M. Beaujuge, *Angew. Chem. Int. Ed.* **2016**, *55*, 12996 –13000.
- [5] Y. Si, X. Zhao, Z. Su, G. Yang, *RSC Adv.* **2016**, *6*, 84705-84711.
- [6] a) B. Pigulski, P. Mecik, J. Cichos, S. Szafer, *J. Org. Chem.* **2017**, *82*, 1487-1498; b) V. V. Meshkovay, A. V. Yudashkin, Yu. N. Klimochkin, *Dyes and Pigm.* **2015**, *113*, 435-446; c) F. Cheng, Y. Yin, G. Zhang, Y. Wang, W. Deng, *Dyes and Pigm.* **2017**, *140*, 222-228; d) S. Mu, K. Oniwa, T. Jin, N. Asao, M. Yamashita, S. Takaishi, *Org. Electron.* **2016**, *34*, 23-27.
- [7] a) E. González-Juárez, M. Güzado-Rodríguez, V. Barba, M. Melgoza-Ramírez, M. Rodríguez, G. Ramos-Ortiz, J.L. Maldonado, *J. Mol. Struct.* **2016**, *1103*, 25-34; b) G. Nam, S. Rangasamy, H. Ju, A. A. S. Samson, J. M. Song, *J. Photochem. Photobiol., B: Biology* **2017**, *166*, 116–125; c) H. Shirani, M. Linares, Ch. J. Sigurdson, M. Lindgren, P. Norman, K. P. R. Nilsson, *Chem. Eur. J.* **2015**, *21*, 15133-15137; d) S. Ying, M. Chen, Z. Liu, K. Zhang, Y. Pan, S. Xue, W. Yang, *J. Mater. Chem. C* **2016**, *4*, 8006-8013; e) A. Goel, A. Sharma, M. Rawat, R. S. Anand, R. Kant, *J. Org. Chem.* **2014**, *79*, 10873-10880; f) S. Sriyab, M. P. Gleeson, S. Hannongbua, *J. Mol. Struct.* **2016**, *1125*, 532-539; g) E. M. A. Al-Imarah, P. J. Derrick, A. J. Patridge, *J. Photochem. Photobiol., A: Chemistry* **2017**, *337*, 82-90; h) S. P. Ponnappa, S. Arumugam, H. J. Spratt, S. Manzhos, A. P. O’Mullane, G. A. Ayoko, P. Sonar, *J. Mater. Res.* **2017**, *32*, 810-821.
- [8] a) R. Mancuso, B. Gabriele, *Molecules* **2014**, *19*, 15687-15719; b) J. Nakayama in *Comprehensive Heterocyclic Chemistry II* (Ed.: C. W. Bird), Elsevier, Amsterdam, **2005**, pp. 607-677; c) F. M. Moghaddama, Gh. R. Bardajeeb, M. Dolabi, *J. Sulfur Chem.* **2010**, *31*, 387–393; d) I. V. Paramonov, N. P. Belskaya, V. A. Bakulev, *Chem. Heterocycl. Compd.* **2003**, *39*, 1385-1388; e) N. P. Belskaya, A. V. Koksharov, A. I. Eliseeva, Z. Fan, V. A. Bakulev, *Chem. Heterocycl. Compd.* **2011**, *47*, 564-570; f) R. S. Giri, H. M. Thaker, T. Giordano, J. Williams, D. Rogers, K. K. Vasu, V. Sudarsanam, *Bioorg. Med. Chem.* **2010**, *18*, 2796-2808; g) C. Heyde, I. Zug, H. Hartmann, *Eur. J. Org. Chem.* **2000**, *19*, 3273-3278; h) A. Noack, H. Hartmann, *Tetrahedron* **2002**, *58*, 2137-2146; i) H. B. Jalani, A. N. Pandya, Dh. H. Pandaya, J. A. Sharma, V. Sudarsanam, K. K. Vasu, *Tetrahedron Lett.* **2012**, *53*, 6927-6930; j) H. Saeidian, A. Saeghi, Z. Mirjafary, F.M. Moghaddam, *Synth. Commun.* **2008**, *38*, 2043-2053.
- [9] a) V. V. Dotsenko, S. G. Krivokolysko, S. V. Shishkina, O. V. Shishkin, *Russ. Chem. Bull.* **2012**, *61*, 2082-2087; b) O. H. Hishmat, A. A. Magd El Din, N. A. Ismail, *Org. Prep. Proced. Int.* **1992**, *24*, 33-37; c) N. P. Belskaya, K. I. Lugovik, A. D. Ivina, V. A. Bakulev, Z. J. Fan, *Chem. Heterocycl. Compd.* **2014**, *50*, 888-900.
- [10] a) E. F. Dankova, V. A. Bakulev, A. N. Grishakov, V. S. Mokrushin, *Russ. Chem. Bull.* **1988**, *5*, 987-989; b) E. F. Dankova, V. A. Bakulev, M. Yu. Kolobov, V. I. Shishkina, Ya. B. Yasman, A. T. Lebedev, *Chem. Heterocycl. Compd.* **1988**, *24*, 1051-1055; c) A. D. Grabenko, P. S. Pel’kis, L. N. Kulaeva, *J. Gen Chem USSR*, **1962**, *32*, 2248; d) M. F. Kosterina, Yu. Yu. Morzherin, A. V. Tkachev, T. V. Rybalova, Yu. V. Gatilov, V. A. Bakulev, *Russ. Chem. Bull.* **2002**, *4*, 653-658.
- [11] a) F. J. Luque, J. M. Lopez, M. Orozco, *Theor. Chem. Acc.* **2000**, *103*, 343–345; b) J. S. Murrey, K. Sen, *Molecular Electrostatic Potential, Concepts and Application*, Elsevier, Amsterdam, **1996**.
- [12] a) H. J. Bohórquez, C. F. Matta, R. J. Boyd, *Int. J. Quant. Chem.* **2010**, *110*, 2418-2425; b) E. R. Johnson, S. Keinan, P. Mori-Sánchez, J. Contreras-García, A. J. Cohen, W. Yang, *J. Am. Chem. Soc.* **2010**, *132*, 6498-6506.
- [13] a) Sh. Sasaki, G. P. C. Drummen, G.-i. Konishi, *J. Mater. Chem. C* **2016**, *4*, 2731-2743; b) T. Stanek, M. Dvorak, N. Almonasy, M. Nepras, I. Sloufova, M. Michl, *Dyes and Pigm.* **2017**, *141*, 121-127; c) M. Szyszkowska, C. Czaplowski, W. Wiczk, *J. Molec. Struct.* **2017**, *1138*, 81-89; d) G. Haberhauer, R. Gleiter, C. Burkhart, *Chem. Eur. J.* **2016**, *22*, 971-978; e) E. Kose, M. Karabacak, F. Bardak, A. Atac, *J. Mol. Struct.* **2016**, *1123*, 284-299; f) A. L. Sobolewski, W. Sudholt, W. Domcke, *J. Phys. Chem. A* **1998**, *102*, 2716-2722.
- [14] W. H. Melhuish, *J. Phys. Chem.* **1961**, *65*, 229-235.
- [15] a) M. Iwaoka, N. Isozumi *Molecules* **2012**, *17*, 7266-7283; b) V. I. Minkin, R. M. Minyaev, *Chem. Rev.* **2001**, *101*, 1247-1265; c) F. T. Burling, B. M. Goldstein, *J. Am. Chem. Soc.* **1992**, *114*, 2313–2320.
- [16] a) A. D. Becke, *J. Chem. Phys.* **1993**, *98*, 5648-5652; b) Y. Zhao, D. G. Truhlar, *Theor. Chem. Acc.*, **2008**, *120*, 215-241; c) T. Yanai, D. P. Tew, N. C. Handy, *Chem. Phys. Lett.* **2004**, *393*, 51-57; d) J. D. Chai, M. Head-Gordon, *J. Chem. Phys.* **2008**, *128*, 084106-1 – 084106-15.
- [17] a) T. H. Dunning, *J. Chem. Phys.* **1989**, *90*, 1007-1023; b) R. A. Kendall, T. H. Dunning Jr., R. J. Harrison, *J. Chem. Phys.* **1992**, *96*, 6796-6806; c) D. E. Woon, T. H. Dunning Jr., *J. Chem. Phys.* **1993**, *8*, 1358-1371; d) K. A. Peterson, D. E. Woon, T. H. Dunning Jr., *J. Chem. Phys.*, **1994**, *100*, 7410-7415; e) A. K. Wilson, T. van Mourik, T. H. Dunning Jr., *J. Mol. Struct.: Theochem.* **1996**, *388*, 339-349; f) S. Grimme, S. Ehrlich, L. Goerigk, *J. Comput. Chem.* **2011**, *32*, 1456-1465.
- [18] J. Tomasi, B. Mennucci, E. Cancès, *J. Mol. Struct.: Theochem.* **1999**, *464*, 211-226.
- [19] A. K. Rappé, C. J. Casewit, K. S. Colwell, W. A. Goddard, W. M. Skiff, *J. Am. Chem. Soc.*, **1992**, *114*, 10024-10035.
- [20] V. Marenich, C. J. Cramer, D. G. Truhlar, *J. Phys. Chem. B* **2009**, *113*, 6378-6396.
- [21] R. Improta, V. Barone, G. Scalmani, M. J. Frisch, *J. Chem. Phys.* **2006**, *125*, 054103-1-054103-9.
- [22] a) V. Barone, *Computational Strategies for Spectroscopy: From Small Molecules to NanoSystems*, Wiley-WCH, Chichester, **2011**; b) B. Mennucci, C. Cappelli, C. A. Guido, R. Cammi, J. Tomasi, *J. Phys. Chem A* **2009**, *113*, 3009-3020.
- [23] a) F. Santoro, R. Improta, A. Lami, J. Bloino, V. Barone, *J. Chem. Phys.* **2007**, *126*, 169903-1; b) F. Santoro, A. Lami, R. Improta, V. Barone, *J. Chem. Phys.* **2007**, *126*, 184102-1-184102-11; c) F. Santoro, R. Improta, A. Lami, J. Bloino, V. Barone, *J. Chem. Phys.* **2008**, *128*, 224311-1-224311-17; d) M. Dierksen, S. Grimme, *J. Chem. Phys.* **2005**, *122*, 244101-1-244101-4; e) H.-C. Jankowiak, J. L. Stuber, R. Berger, *J. Chem. Phys.* **2007**, *127*, 234101-1-234101-23; f) R. Borrelli, A. Capobianco, A. Peluso, *Can. J. Chem.* **2013**, *91*, 495-504.
- [24] C. M. Breneman, K. B. Wiberg, *J. Comp. Chem.* **1990**, *11*, 361-373.
- [25] a) F. W. Biegler-König, R. F. W. Bader, T. H. Tang, *J. Comput. Chem.* **1982**, *3*, 317–328; b) AIMPAC, <http://www.chemistry.mcmaster.ca/aimpac/imagemap/imagemap.htm>; c) N. Keith, Ph.D. Thesis, Ontario, Canada, **1993**.

For internal use, please do not delete. Submitted Manuscript

FULL PAPER

Entry for the Table of Contents

FULL PAPER



Kseniya I. Lugovik, Alexander K. Eltyshev, Enrico Benassi, * Nataliya P. Belskaya*

Page No. – Page No.

New Promising Method for the Challenging Synthesis of 5-Acyl-2-Amino-3-Cyanothiophenes: Chemistry and Fluorescent Properties

An efficient method for the synthesis of new polyfunctional thiophenes is reported. Quantum mechanical calculations provide the explanation of the synthetic pathway of this heterocyclization. Both experimental and computational spectral results demonstrate that the particularities of the optic properties synthesized thiophenes are caused by the presence of an ICT state during absorption and a TICT state after geometry relaxation in the excited state.